Seabed mapping and characterization of sediment variability using the usSEABED database

John A. Goff[1], Chris J. Jenkins[2], and S. Jeffress Williams[3]

[1]Institute for Geophysics, Jackson School of Geosciences, University of Texas at Austin, Austin, TX 78758 USA (goff@utig.ig.utexas.edu)

[2]INSTAAR, University of Colorado, Boulder CO 80309-0450 USA (chris.jenkins@colorado.edu)

[3]U.S. Geological Survey, Woods Hole Science Center, Woods Hole MA 02543 USA (jwilliams@usgs.gov)

Submitted to Continental Shelf Research, March, 2007

Abstract. We present a methodology for statistical analysis of randomly-located marine sediment point data, and apply it to the U.S. continental shelf portions of usSEABED mean grain size records. The usSEABED database, like many modern, large environmental datasets, is heterogeneous and interdisciplinary. We statistically test the database as a source of mean grain size data, and from it provide a first examination of regional seafloor sediment variability across the entire US continental shelf. Data derived from laboratory analyses ("extracted") and from word-based descriptions ("parsed") are treated separately, and they are compared statistically and deterministically. Data records are selected for spatial analysis by their location within sample regions: polygonal areas defined in ArcGIS chosen by geography, water depth, and data sufficiency. We derive isotropic, binned semivariograms from the data, and invert these for estimates of noise variance, field variance, and decorrelation distance. The highly erratic nature of the semivariograms is a result both of the random locations of the data and of the high level of data uncertainty (noise). This decorrelates the data covariance matrix for the inversion, and largely prevents robust estimation of the fractal dimension. Our comparison of the extracted and parsed mean grain size data demonstrates important differences between the two. In particular, extracted measurements generally produce finer mean grain sizes, lower noise variance, and lower field variance than parsed values. Such relationships can be used to derive a regionally-dependent conversion factor between the two. Our analysis of sample regions on the U.S. continental shelf revealed considerable geographic variability in the estimated statistical parameters of field variance and decorrelation distance. Some regional relationships are evident, and overall there is a tendency for field variance to be higher where the average mean grain size is finer grained. Surprisingly, parsed and extracted noise magnitudes correlate with each other, which may indicate that some portion of the data variability that we identify as "noise" is caused by real grain size variability at very short scales. Our analyses demonstrate that by applying a bias-correction proxy, usSEABED data can be used to generate reliable interpolated maps of regional mean grain size and sediment character.

Keywords: grain size; continental shelf; database; semivariogram; statistical analysis; kriging

1. Introduction

The physical properties of seafloor sediments on the continental shelf are spatially variable on many scales due to a complex underlying geologic framework and seafloor processes: from regional-scale variations (10 to 100 km), such as those associated with proximity to major depocenters or the shoreline, down to mesoscale variations (1 to 10 cm), such as those associated with ripple bedforms. In between are variations associated with a multitude of bedform types and scales (e.g., sand ridges, rippled scour depressions, dunes, megaripples, ribbons), reworking and erosion, or patchiness caused by such factors as localized erosion, biologic processes (e.g., shell patches), bedrock outcrop, or glacial detritus (gravel patches). Spatial variability is related to process, and we seek, ultimately, to achieve a basic understanding of the geological response to the oceanographic and sedimentological processes acting on the seafloor. We seek as well to utilize that relationship as a predictive tool. In other words, if we understand the seabed environment sufficiently, can we make reliable predictions about the quantitative characteristics of sediment variability? Such a capability would have important applications in, for example, ocean acoustics, where regional seabed variability strongly affects acoustic response over long path lines (e.g., Lapinski and Chapman, 2005), or benthic habitats, where environmental heterogeneity is a particularly strong predictor of species richness (e.g., Kerr et al., 2001). Quantitative understanding of seafloor variability at all scales is also important for map making, in particular for applying techniques that reduce data uncertainty (Goff et al., 2006), and for geostatistical interpolation (e.g., kriging; Cressie, 1990).

Data quantity and coverage are the most significant challenges to investigating the variability of seafloor sediments. Spatial variability is a statistical measure of ensemble properties, quantified by such functionals as the power spectrum, covariance function or semi-variogram.

Robust estimation of these types of functions requires large quantities of data sampled over a large range of spatial scales. However, that is very difficult to obtain. Despite years of advances in acoustic remote sensing (e.g., Pratson and Edwards, 1996), and increased sophistication of classification algorithms (e.g., Atallah and Probert Smith, 2004; Bartholomä, 2006), characterizing the physical properties of seafloor sediments remains a significant challenge. For example, although acoustic backscatter data are strongly related to sedimentary properties, the number of potential variables affecting backscatter are so large as to make the problem of seabed discrimination exceedingly difficult (e.g., Jackson et al., 1986; Ferrini and Flood, 2006). Furthermore, the seabed factors of greatest importance in determining backscatter appear to be very local in scope (e.g., Goff et al., 2000; 2004), so that global algorithms for determining sedimentary character from backscatter data will likely perform poorly. It remains necessary to directly sample sediments in order to measure properties consistently from one region to another. Unfortunately, direct sampling is very time consuming and expensive and, even with extensive effort, often results in a relatively small number of sample sites for any single field campaign.

The issue of comprehensive data coverage of seabed samples for the U.S. continental margins is being addressed in a collaborative research effort between the U.S. Geological Survey and INSTAAR at the University Colorado (usSEABED; Williams, et al., 2003; Reid et al., 2005, 2006; Buczkowski et al., 2006). This work has resulted in a database methodology for assembling extant seabed observations (dbSEABED; Jenkins, 1997, 2002). Extensive effort has gone into collecting, evaluating, assembling, and publishing available records within published and unpublished data sets from federal and state agencies, universities, industry and individual researchers. The result is a combined U.S. database of such observations (Figure 1). Although coverage is far from uniform and is based on surveys spanning approximately the past 120 years, these collections provide, in many continental shelf and estuarine regions, a data set that is sufficient in quantity and coverage to robustly map seabed properties and to estimate spatial variability functions such as the semi-variogram. The usSEABED database is a unique resource that would not be possible to collect by individual investigators. The methods employed in the usSEABED project relate to a growing and necessary computational resource in environmental sciences: large aggregated, heterogeneous and interdisciplinary data bases (e.g., Osenberg et al. 1999; Jones et al. 2006).

Our primary goal for this paper is to statistically test the viability of the heterogeneous usSEABED database for mapping seabed properties and for investigating sediment variability on the seafloor. This is a test case for wider application to worldwide coverage. To maintain focus in our analysis, we will restrict consideration to mean grain size measurements of unconsolidated sediments (i.e., no outcrop observations) in an open-ocean (i.e., no estuary observations), continental shelf setting. Mean grain size is a commonly reported measurement in the dbSEABED databases, which provides a good opportunity to maximize data content in any given area. Mean grain size can also be related to other important physical parameters, such as bulk density, seismic velocity, and sediment transport potential (e.g., Stoll, 1977; Hamilton and Bachman, 1982; Ogushwitz, 1985).

Our secondary goal is to employ the results of our analysis in a preliminary investigation of variability as a function of geography and, to the extent warranted by the data, water depth. At this exploratory stage in our investigation we seek first to obtain an overall view of what sediment variability looks like on the US continental shelf. Future investigations, probably requiring a larger, global database, may seek to answer more refined questions regarding the relationship of sediment variability to environmental parameters such as shelf slope, shelf width, wave climate, proximity to sources/sinks, etc. The data employed here primarily permit only regional interpretations. More detailed investigations, e.g., ground-truthing sonar backscatter maps, would require extensive additional sampling. However, the methodology we describe can be used on small or large spatial scales to integrate data from multiple sources.

While our primary goal may, on first consideration, appear straightforward, in reality it presents significant and important challenges owing to the heterogeneous nature of the data base. The usSEABED data base holds data that were collected by a large number of different investigators at different times utilizing a range of methodologies. The issues that arise also appear in aggregated bathymetric datasets of the seafloor (e.g., Jakobsson et al., 2002; Calder, 2006). In the case of the usSEABED data base these issues are of particular relevance:

(1) Mean grain sizes are reported in two fundamentally different ways: “extracted” and “parsed”. Extracted data are computed from grain size histograms determined by precise analytical means (e.g., sieves, settling tubes, diffractometry). Parsed data are inferred through a conversion by means of a fuzzy set theory (Zadeh 1965) of visual descriptions (i.e., including coarse, medium or fine sand, gravel, silt, mud, clay, shells, etc.). Such inferences are less precise, but in many regions constitute the majority of the data coverage and in some cases the only data available.

(2) Parsed and extracted mean grain size measurements perform differently in various parts of the grain size spectrum with respect to accuracy and precision. For example, while analytic methods can accurately measure grain size contributions from ~10mm to 2μm, visual descriptions are limited to grain sizes above ~20μm, and so have lower accuracy in the fine grain sizes (silt and finer).

(3) Laboratory analyses of sediment grain size histograms sometimes exclude shell and gravel contents, and other difficult-to-treat components. This happens typically when a researcher is primarily interested in sediment transport or physical properties issues, and does not consider the shell content germane to the research (e.g., Poppe, et al., 2001; Moore et al., 2002). Visual descriptions typically do represent the presence of shell and gravel when it is present, hence a bias may arise between parsed and extracted determinations of mean grain size.

(4) Data within usSEABED are collected across several decades in most regions, so that temporal variability may be superimposed on spatial variability. In addition, navigational uncertainties have changed markedly through the years, from >1 km for old star fixes and LORAN-navigated data, to < 100 m for satellite navigation, to < 10 m for GPS. Large uncertainties can lead to juxtaposition of different types of sediment where the natural heterogeneity is strong. At present, temporal information cannot be extracted from the usSEABED database.

Our challenge is to utilize this complex data set in a coherent and consistent manner, and to properly characterize uncertainty and bias in each of the types of data included in it. Many readers may question *a priori* the value of treating quantitatively a data set which is subjective by its very nature. But the value lies in the statistics of large numbers: a single estimate of mean grain size from a visual description may have little credibility, but many such estimates, when considered as an ensemble, can. In this paper we establish that credibility by demonstrating a quantitative, statistical relationship between the word-based and analytically-derived estimates of mean grain size.

2. Methods

2.1. Derivation of mean grain size from observations and samples

The dbSEABED software deals with both analytical (numeric) and descriptive (word-based) data types, which pass outputs that are termed “extracted” and “parsed”, respectively. Extracted mean grain size values are derived with minimal processing from the original records, whereas parsed values are formulated via recognition of the linguistic parts of sediment description leading to analysis of the meaning (e.g., Grune and Jacobs, 1990). Here we employ ϕ grain size units, where $\phi = -\log_2$[mm size] (gravel is -8 to -1ϕ, sand is -1 to 4ϕ, and mud is 4 to 12ϕ)

In the extraction stream of processing, we begin by nominating a standard (moment mean) to which other measures of grain size must conform, or be made to conform with, to be accepted as inputs. Those various measures include: median, Folk (1974) and Inman (1952) graphic ‘means’, geometric mean, and mode. The conformance of these measures is revealed by cross-comparisons using data collections of over 10,000 samples (including, for example, Poppe et al., 2005) where two or more have been determined together (Figure 2). The Folk and Inman graphic means do conform (and are acceptable as input), but modes do not (and are unacceptable). Conformance to the moment mean standard can be improved during processing using an adjustment on the incoming data (e.g., Smith and McConnaughey, 1999).

In many datasets, analytic determinations of detailed grain size histograms are available instead of the mean value. In these circumstances, the moment mean grain size is calculated directly from the histogram. We have implemented a set of filters to reject analyses which purport to be of the entire sediment, but are actually limited to a certain instrumentation and fraction (e.g., to sand in the case of settling columns). Where a sediment mean grain size is reported in the data in addition to detailed grain size histogram, the reported mean takes precedence.

The possibility of a bias in analytical measures of mean grain size is raised because common practice for many investigators is to remove all carbonate content, including coarser shell hash, from a sample prior to analysis. This practice is highlighted in the USGS manual on grain size analysis (Poppe et al., 2001):

> Whole or fragmented calcite secreting micro- and macro-organisms can bias the grain size distribution if they occur in significantly high concentrations. Because biogenic carbonates commonly form *in situ*, they usually are not considered to be hydraulically representative of the depositional environment from a textural standpoint (Reineck and Singh, 1980). Their presence alters the textural data and complicates interpretation. ... If limited to the gravel fraction, it is often easier to manually remove the fragments of bivalve shells and other biogenic carbonate debris ....

The reportage, or not, of shell material as part of the sample analysis is therefore a point-of-view issue. For purposes of hydraulic analysis, shells are considered unrepresentative of the processes under consideration, and so are simply ignored. For other purposes, such as understanding acoustic backscatter, the presence of shells can be a critical factor (e.g., Goff et al., 2004). Over the entire usSEABED database, however, it is important to consider the possibility of a bias in analytic measures of mean grain size due to the under-reportage of shell material.

Word-based data are treated with an algorithm which parses (recognizes) and analyzes (comprehends) text descriptions of the sediments and compiles an estimated grain size using fuzzy set theory memberships for lithologic and size terms (Jenkins, 1997). The input descriptions are held in original, although abbreviated terms. With the use of pointers and some special syntaxes, potential ambiguities in descriptions are resolved. Functional roles for terms as (geological material) objects, (property) modifiers, quantifiers and locators are recognized from the dictionary. A dictionary, organized as thesaurus, provides numeric and coded meanings to each term. Terms may be relevant/irrelevant and known/unknown in meaning for each parameter (e.g., for grain size respectively: “fine sand” / “green”, and “fine sand” / “sediment”). The numeric meanings, including the grain size characteristics of described components, are assembled in a linear weighting scheme (Jenkins, 1997, Fig. 2). During processing the unknown parts are monitored and, if above 5%, the parsing is aborted. Any term not in the dictionary also causes an abort. More information on the parsing process is given in Jenkins (1997, 2002), Reid et al. (2005, 2006), and Buckzowski et al. (2006).

Opportunities exist in the process to monitor how well the parser is performing. We use those samples where word-based and measured analytical data are both available. A recent calibration using 10,029 usSEABED samples yielded a correlation coefficient of +0.59 between extracted and parsed mean grain size values. Across the same dataset (Figure 3) the median average deviation was 0.9 ϕ. The ranges of confidence at 1σ and 2σ were 1.25 and 4.2 deviation in absolute ϕ.

2.2 Data preparation and sampling

Prior to statistical analysis, we process the mean grain size data in two ways: (1) “culling,” which eliminates redundancies at any specific location and restricts consideration to only seafloor samples of unconsolidated sediments, and (2) definition of polygonal sample areas which restrict consideration to only samples that fall within areas that they define. Culling is required because usSEABED records frequently list multiple entries with identical coordinates. This can occur with repeat measurements on a single surface sample, but also when different subbottom samples are analyzed, such as from cores. We restrict consideration to “seafloor” samples by excluding those whose bottom depth entry in the usSEABED database is greater than

0.5 m below the seafloor. Where we did encounter multiple seafloor grain size measurements at a single location, they were simply averaged. Parsed and extracted measurements of mean grain size are kept in separate data files, so that one type of measurement does not exclude the other where both are made at the same location. We also restrict consideration to observations from unconsolidated sediments. "Hard ground" observations (exposures of old, lithified material) do not fit within the mathematical framework of mean grain size measurements. A complete statistical treatment of seafloor terrains with outcrop exposures would require separate characterization of both the unconsolidated sediments and the binary hard ground/soft ground relationship. Such a treatment is beyond the present scope, but could readily be incorporated if required for some applications. An example of statistical characterization of a binary field can be found in Goff et al. (1994).

We define sample areas for statistical analysis to investigate geographic changes in sediment variability. Choosing sample areas necessarily involves a balance among two competing factors: geographic and statistical resolution. Geographic resolution is maximized by minimizing the size of sample areas. Conversely, statistical resolution is maximized by increasing the number of samples, which, given a preexisting data set, requires increasing the size of the sample area. As a rule-of-thumb, we found that having at least 1000 well-distributed (i.e., not all clumped together) samples in a sample area resulted in a semi-variogram estimate that was well-enough resolved (i.e., not overly erratic) to obtain stable statistical parameter estimates; we used this as a guiding factor for choosing the size of sample regions. This is not a hard-and-fast rule, however. A region with fewer samples may be chosen if tolerance for statistical inaccuracy is higher, or if, by enlarging the area further, one would unduly risk combining overly different geographic environments into a single estimate. Some areas simply have too-few samples in them to include in this analysis; this includes large portions of the Pacific and Gulf of Mexico shelves. Other than sample size, we also considered major geographic features (e.g., Cape Hatteras, NC or Cape Cod, MA) and, where data coverage provided adequate support, water depth in defining sample area boundaries. Jenkins and Goff (2007), in a statistical analysis of mean grain size data in the Adriatic Sea, separated the data by depth values and found that statistical parameters changed markedly across the 20-m isobath. For the usSEABED database, only the Atlantic shelf afforded sufficient coverage to utilize water depth to define sample areas. For those data, we also use the 20-m isobath as a boundary, as well as the 50-m and 100-m isobaths to distinguish between inner, middle and outer continental shelf sample areas. Overall we defined 31 sample areas for the usSEABED database in U.S. continental shelf waters (19 in the Atlantic, 6 in the Gulf of Mexico, and 6 in the Pacific).

ArcGIS (Ormsby et al., 2001) was used to define polygonal sample areas, and then to select usSEABED data points within those areas for statistical analysis. An example from the mid-Atlantic Bight is presented in Figure 4. We first import a freely-available US political boundary shape file to define the coastline. Bathymetry is extracted from the NOAA (2007) Coastal Relief Model directly into an ArcGIS-compatible grid format. Upon loading the bathymetry into ArcGIS, we use the contour tool (in the spatial analyst tool box extension) to determine the 20, 50, and 100 m contours for display. These are subsequently used to guide our choice of polygonal sample areas. The culled usSEABED mean grain size values, both parsed and extracted, are loaded into ArcGIS for display. Polygonal areas are then defined within a new shape file using the interactive graphics capabilities of ArcGIS. In the example shown in Figure 4, the Hudson Shelf Valley was excluded from the sample areas because it is, in essence, a geologic province unto itself: an anomalous region of fine grained sediments that is a result of the unique presence of the shelf valley across the continental shelf morphology (Vincent et al., 1981; Harris et al., 2003). Figure 5 displays all the sample areas defined on the continental shelf for the usSEABED database, color coded by the average mean grain size of the parsed records in those areas. The areas are identified numerically for reference to Table 1, which lists grain size statistics for each region derived in the following sections.

2.3 Semivariogram analysis of data field

2.3.1 Computation of the semi-variogram

The semivariogram is a common tool for geostatistical characterization of a data field (e.g., Deutsch and Journel, 1992; Christakos, 1992). As a function of lag vector, **L**, the semivariogram $S(\mathbf{L})$ is defined by:

$$S(\mathbf{L}) = \frac{1}{2} E\left[\left(d(\mathbf{L}) - d(\mathbf{X}+\mathbf{L}) \right)^2 \right], \qquad (1)$$

where E[] is the expected value, and $d(\mathbf{x})$ is a zero-mean data value at location **X**. In practice, we typically remove a trend field from the data over a sample area by fitting a bilinear surface (Wessel and Smith, 1998) to the data and subtracting it. Equation (1) assumes that the field is statistically homogenous; i.e., that statistical properties are not a function of **X**. Removal of a trend surface, as described previously, helps to enforce this assumption. The semivariogram is related to the covariance function $C(\mathbf{L})$ by the simple relationship $S(\mathbf{L}) = H^2 - C(\mathbf{L})$, where H^2 is the field variance.

Although this paper is focused on situations where the field data are randomly (meaning: not located on a regular grid) and sparsely located in space, it is instructive to first consider the formulation for estimating the discrete semivariogram from field data $d_{i,j}$ that are sampled fully on an N_x by N_y grid, with x and y increments Δx and Δy and coordinates indexed by (i,j): $1 \leq i \leq N_x$; $1 \leq j \leq N_y$:

$$\hat{S}_{k,l} = \frac{1}{2(N_x - k)(N_y - l)} \sum_{i=1}^{N_x} \sum_{j=1}^{N_y} (d_{i,j} - d_{i+k,j+l})^2 , \tag{2}$$

where the lag vector is defined by $\mathbf{L} = (k\Delta x, l\Delta y)$. The semivariogram (or covariance) estimated in this way is generally a smoothly-varying function by virtue of the fact that proximal values are highly correlated with each other (Goff and Jordan, 1989). This can be understood intuitively by recognizing that, for example, the formulas for $\hat{S}_{k,l}$ and $\hat{S}_{k,l+1}$ utilize nearly all the same $d_{i,j}$ values, and the $d_{i+k,j+l}$ values are likely to be only slightly different from the $d_{i+k,j+l+1}$ values.

Estimating the semivariogram from randomly-located data is not as straightforward; it must be accomplished with a binning method. In addition, sufficient support of two-dimensional characterization of the semivariogram from generally sparse, randomly-sampled data is generally not available. We therefore restrict our attention here to the isotropic, one-dimensional semivariogram, which is a function of the lag distance $L = |\mathbf{L}|^2$. We define bins using a bin size ΔL, where the k^{th} bin is defined by the range $(k\text{-}1)\Delta L \leq L < k\Delta L$. Assume we have randomly-located field data points, $d(\mathbf{X}_i)$, $i \in 1,N$, in a sample area. We express the semivariogram estimation via:

$$\hat{S}_k = \frac{1}{N_k} \sum_{i=1}^{N} \sum_{j=1}^{N} I_{i,j}(k) d(\mathbf{X}_i) d(\mathbf{X}_j) , \tag{3}$$

where

$$I_{i,j}(k) = \begin{cases} 1, & (k-1)\Delta L \leq |\mathbf{X}_i - \mathbf{X}_j| < k\Delta L \\ 0, & \text{otherwise} \end{cases} \tag{4}$$

and

$$N_k = \sum_{i=1}^{N} \sum_{j=1}^{N} I_{i,j}(k) \, . \tag{5}$$

An example semivariogram estimated from a sample area of the Atlantic usSEABED database, computed using equations (3)-(5), is displayed in Figure 6. Here and elsewhere we employ a lag bin size ΔL of 200 m. For most regions we examined, this bin size typically results in bin populations (determined by the number of point pairs whose lag distance falls within the bin) of ~1/2 to 2 times the total data population of the region (although fewer at the shortest lag distances). A defining characteristic of this and all other such examples is the very high level of erraticity (i.e., strong variability from one discrete lag value to the next). This observation stands in sharp contrast to smoothly-varying semivariograms typically derived from regularly-sampled data using equation (2). The fundamental reason for this behavior is that the values of $\hat{S}_k$ are highly uncorrelated with each other. This is, in part, a direct consequence of the sparse, random sampling: heuristically it is evident in equation (3) that $\hat{S}_k$ and $\hat{S}_{k+1}$ will be computed using very different sets of data values, rather than very similar sets as in equation (2) for regularly sampled data. The value N_k is itself a random number, which can change substantially from one lag index to the next. High levels of data uncertainty (noise) can also contribute significantly to the erraticity of the semivariogram.

2.3.2 Parameter estimation

We estimate second-order statistical properties of the data field through an iterative, weighted, least-squares inversion of the semivariogram (e.g., Menke, 1989). Following the notation of Menke (1989), we define **d** as the "data" vector of semivariogram estimates $\hat{S}_k$, $\mathbf{m}_n^{est}$ as the vector of model parameters at the n^{th} iteration, and $\mathbf{g}(\mathbf{m}_n^{est})$ as the vector of model predictions from those parameters. The iterative, linearized inversion formulation is then expressed as:

$$\mathbf{m}_{n+1}^{est} = \mathbf{G}_n^{-g}(\mathbf{d} - \mathbf{g}(\mathbf{m}_n^{est})$$

$$\mathbf{G}_n^{-g} = \mathbf{G}_n^{\mathrm{T}}[\mathrm{cov}\,\mathbf{d}]^{-1}\mathbf{G}_n, \tag{6}$$

where cov **d** is the covariance matrix of the data vector, and the sensitivity matrix $[\mathbf{G}_n]_{ij} =$ $\partial g_i / \partial m_j$ is evaluated at $\mathbf{m}_n^{est}$.

We fit the one-dimensional, semivariogram form of the von Kármán statistical model (e.g., Goff and Jordan, 1988), with white noise variance, N^2, added. In discrete form, where $L = k\Delta L$, this can be written as

$$S(k\Delta L) = N^2 + H^2\left[1 - G_\nu(Kk\Delta L)/G_\nu(0)\right], \tag{7}$$

where K is a lag scale parameter and the G_ν is defined by

$$G_\nu(r) = r^\nu K_\nu(r), 0 \le r < \infty, \nu \in [0,1]. \tag{8}$$

K_ν is the modified Bessel function of the second kind of order ν. G_ν are a class of monotonically decaying functions (see plots in Goff and Jordan, 1988). There are four model parameters to be fitted: N^2, H^2, K and ν. In geostatistical terminology, N^2 represents the "nugget" of the semivariogram, and $N^2 + H^2$, the maximum value reached with increasing lag, is the "sill." The order parameter ν primarily controls the behavior of $G_\nu(r)$ at the origin; its slope at $r = 0$ is zero for $\nu = 1$ and infinite for $\nu = 0$. $G_{1/2}(r)$ is simply an exponential function. The Hausdorff (fractal) dimension D of a topographic surface can be related to the asymptotic properties of the covariance/semivariogram function at small lag (Adler, 1981). The Hausdorff dimension associated with Equation (7) is D = 2 − ν for profiles and 3 − ν for surfaces (Goff and Jordan, 1988).

The lag scale parameter, K, largely determines how quickly the field decorrelates with increasing lag (i.e., how quickly the semivariogram approaches the sill), although the order parameter also has an influence. A decorrelation length, λ, can be defined by the width (second moment) of the covariance (Goff and Jordan, 1988):

$$\lambda = \frac{2\sqrt{2(\upsilon + 1/2)}}{K}. \tag{9}$$

The decorrelation length is a physically intuitive parameterization of the approximate width of the principal structures of the field.

Partial derivatives for the covariance form of the von Kármán were calculated by Goff and Jordan (1988; 1989), and are easily converted to the semivariogram form of the model.

The weighted inversion formulation also requires identification of a data covariance matrix (cov **d** in Equation 6), which involves defining the fourth moment of the field data (Goff and Jordan, 1989). This is a tractable computation for regularly sampled data, but becomes very difficult for randomly located data. However, we infer from our observation that these semivariograms are highly erratic, and we can reasonably assume that the data points are largely uncorrelated with each other. We thus approximate the data covariance with a diagonal matrix, where the elements are defined by the semivariogram error variance. We estimate these elements empirically, employing two metrics: (1) the variance of the misfit between the semivariogram estimated from the data and the semivariogram model, which is iteratively reduced during the least-squares inversion procedure, and (2) the number of data pairs, N_k, that are used to estimate the k^{th} semivariogram bin. The error variance for the bin average is expected to be proportional to the inverse of the number of sample points for that bin. We define E_A^2 as the average error variance,

$$E_A^2 = \frac{1}{N_b}\sum_{k=1}^{N_b}(\hat{S}_k - S(k\Delta L))^2\,, \tag{10}$$

where N_b is the number of semivariogram estimation bins, and $S(k\Delta L)$ is the model function defined in Equation (7), updated iteratively by the inversion Equation (6). We further define N_A as the average number of bin samples:

$$N_A = \frac{1}{N_b}\sum_{k=1}^{N_b} N_k \tag{11}$$

The bin error variance is then estimated via

$$E_k^2 = E_A^2 \frac{N_A}{N_k}\,, \tag{12}$$

and these values are used to define the diagonal elements of the semivariogram covariance matrix. We often find that the lowest lag values of the semivariogram are highly erratic owing to a scarcity of samples in those bins. The bin error formulation of Equation (12) sufficiently reduces the weight of such values so that they do not adversely affect the inversion result.

The erratic nature of the semivariograms estimated from randomly located data unfortunately make accurate estimation of the ν parameter (i.e., the fractal dimension) a nearly impossible task, in that the inversion quickly becomes unstable. The value of ν typically needs to be fixed to enable stable estimation of the other parameters, and for these data examples we choose $\nu = 0.5$ (fractal dimension of 1.5 for a profile, 2.5 for a surface), which is identical to an exponential model.

Figure 6 demonstrates a best-fit semivariogram model employing the method described above. The inversion formulation also provides estimates of the errors on model parameters (Menke, 1989):

$$[\mathrm{cov}\,\mathbf{m}^{est}] \cong \mathbf{G}_n^{-g}[\mathrm{cov}\,\mathbf{d}]\mathbf{G}_n^{-g\mathrm{T}}\,. \tag{13}$$

However, errors computed by this formulation must be considered underestimates because our assumption of uncorrelated semivariogram estimates is not strictly correct. Realistic 1-σ errors for N^2 and H^2 are ~10% of the sill value (the sum of N^2 and H^2), and for decorrelation length are ~25-50% (generally increasing with the decorrelation length).

3. Extracted vs. Parsed mean grain size value comparison

Our most fundamental issue in utilizing the usSEABED database mean grain size values is the comparability of extracted and parsed forms of measurements. In this section, we make two forms of comparison: (1) a direct comparison of proximal values, and (2) comparison of statistical parameters in sample areas that are well-covered by both record types.

3.1 Direct comparison of proximal values

We form extracted/parsed mean grain size pairs for comparison by finding, for each extracted measurement, the nearest parsed measurement no greater than 200 m away. No comparison is made for pairs greater than 200 m distant. More than 6,900 such proximal comparisons can be made over the entire usSEABED database (Figure 7), many of which are collocated. Figure 7 displays a significant amount of scatter, but nevertheless indicates a positive relationship between the two types of measurements of mean grain size. To better characterize this relationship, we have averaged the plotted points in two ways: (1) for each 1-ϕ extracted bin, we have determined the average parsed mean grain size, and (2) for each 1-ϕ parsed bin, we have determined the average extracted mean grain size. The vast majority of samples fall within the range ~1-7 ϕ, and within this range both forms of averaging consistently indicate that parsed measurements tend to have lower ϕ values (coarser mean grain sizes) than extracted measurements, typically by ~0-1 ϕ. This indicates a bias in one of the two measurement types.

The average extracted/parsed bin averages diverge, however, at both ends of the ϕ scale. At the upper end (finer grain size), extracted mean grain sizes reach values as high as 10 ϕ, whereas the parsed mean grain sizes are limited to ≤ 7 ϕ. This can be explained by the fact that the presence of "clay" (≤ 8 ϕ) cannot be verified in visual observations. Analytic methods, however, are able to discern finer grain sizes. At the lower end (coarser grain sizes), we observe that low-ϕ parsed measurements are generally not matched by low-ϕ extracted measurements, and likewise that low-ϕ extracted measurements are not generally matched by low-ϕ parsed measurements (although there are far more examples of the former than the latter). The disparities worsen with decreasing ϕ (increasing grain size). We can envision two possible explanations for this observation: (1) that gravel/shelly patches tend to be spatially very confined, so that even proximal measurements can have large disparities, or (2) that the reporting of the gravel portion of samples in the usSEABED records is not very consistent, and worse for extracted measurements than for parsed measurements although examples of each are probable.

3.2 Comparison of statistical parameters

Of the 31 sample areas defined for the usSEABED database, 12 had sufficient coverage (see discussion in Section 2.2) of both parsed and extracted mean grain sizes to robustly estimate the variogram for inversion of statistical parameters. Figure 8 shows three such comparisons with contrasting results. Figure 8a presents what may be considered the ideal situation: the semivariograms estimated from both parsed and extracted mean grain sizes are nearly identical in shape, as evidenced by the similarity of the field variance and decorrelation length parameters. The only substantive difference between the two is that the level of noise variance is higher in the semivariogram estimated from the parsed data, in accordance with expectations.

Figure 8b presents a situation where the field variance is much larger for the parsed data than it is for the extracted data. Otherwise, as with Figure 8a, the decorrelation lengths are very similar, and parsed data exhibit greater noise variance. The difference in field variance could have a number of causes, including the possibility that coarse fractions are under-reported for the extracted data.

Figure 8c presents a third different case: here the field variance of the extracted mean grain sizes are much larger than for the parsed data. On the other hand, the "sill" value (the maximum value approached by the semivariogram) of the parsed semivariogram is ~1 ϕ^2 larger than for the extracted semivariogram, and the noise variance of the parsed data is much larger than can be reasonably explained by data uncertainty. The evidence here suggests that a significant portion of the true field variance in the parsed data is being expressed as uncorrelated (noise) variance. The reasons for this are not clear, but could be related to spatial undersampling of real features or to location uncertainty in older data sets.

The primary lesson to be learned from the examples shown in Figure 8 is that the relationship between parsed and extracted measurements of mean grain size cannot be determined on a national or global scale, but rather must be determined on a case-by-case, region-by-region basis. Nevertheless, it may be possible to utilize these sorts of comparisons to formulate a local conversion factor between the two types of data measurements.

Figure 9 displays graphs of parsed versus extracted statistical parameters (including the average mean grain size) for the 12 sample areas well covered by each type of data. In the comparison between average mean grain sizes (Figure 9a), we again observe the tendency, noted in Figure 7, for the parsed values to be less than the extracted values. Otherwise the averaged mean grain size for the regions are strongly correlated (correlation coefficient of +0.89, with confidence >99%). In the comparison of field variance (Figure 9b), we find at the lower values a tendency for the parsed values to increase faster than the extracted values. That trend appears to reverse, however, at the larger field variance values. On the other hand, the two largest field variances for the extracted samples, one of which is the example shown in Figure 8c, correspond to the two anomalously large noise variances in the parsed data (Figure 9c). If, as we argued earlier, these sample areas are cases where a significant amount of the parsed field variance is being expressed as noise variance, then these two anomalous values in Figure 9b would plot much closer to the 1:1 line (correlation coefficient of +0.83, with confidence = 97%). Aside from these two anomalous values, the noise variances in Figure 9c display a clear pattern of larger parsed values than extracted values (average difference 0.43 ϕ^2), and furthermore exhibit a strong positive correlation between parsed and extracted noise variances (correlation coefficient of +0.80, confidence = 99%). We will consider the causes for this correlation, which is unexpected, in the following section. The decorrelation lengths (Figure 9d) display considerable scatter, as befits the least well-resolved statistical parameter, but generally display a positive correspondence between the two types of measurements (correlation coefficient +0.54, with confidence = 99%) with no obvious biases.

4. Results of statistical analysis

Our estimates of field variance and decorrelation length scale within the usSEABED continental shelf sample areas (Figure 5) are listed in Table 1 and summarized graphically in Figures 10 and 11, respectively. In sample areas for which we were able to obtain estimates from both parsed and extracted data records, the higher of the two field variance values were used for display in Figure 10. As noted earlier and in Figure 9b, most of the higher field variances were recorded with the parsed data, and we speculate is largely due to under-reportage of coarse fraction in analytic methods used for the extracted data. The two primary exceptions (Figure 9b) are those where an unrealistically large portion of the total parsed field variance is accounted for by the noise variance, and in these cases we assume that the larger field variances from the extracted data are more representative. For the display of decorrelation length scales in Figure 11 we average the values from parsed and extracted data sets in regions where both are estimated, weighted by the number of samples of each. Geographically, we can use these plots to make several important observations:

(1) While the carbonate sands of the southeast and southwest Florida shelf and the siliciclastic sands of the U.S. Atlantic shelf south of Cape Cod are both among the largest overall mean grain sizes (Figure 5), they present strongly contrasting statistical behaviors. The grain size variance (Figure 10) of the Florida shelf is relatively large (~1.5-3 ϕ^2), and the decorrelation lengths (< 8 km; Figure 11) are among the shortest observed. With the exception of regions just north of Cape Hatteras, the U.S. Atlantic shelf sediments exhibit low variance (< 1 ϕ^2; Figure 10), and a large range of decorrelation lengths (Figure 11). There is no evident relationship between decorrelation distance and water depth, in contrast to the observations of Jenkins and Goff (2007) for the sediments of the Adriatic sea. The high variance and short decorrelation

scales on the Florida shelf imply that there is less spatial predictability in these sediments than most anywhere else. Short-scale patchiness of shell beds may be a contributing factor. By contrast, the U.S. Atlantic shelf exhibits some of the highest grain size predictability (not counting "hard-ground" outcrops, such as are know to be present on the Carolina shelf, for example; Thieler et al., 1995), owing to the low variances and larger decorrelation length scales.

(2) Finer-grain size regions appear to exhibit moderate to large variances. The sediments off Cape Cod and within the Gulf of Maine, which are strongly influenced by glacial detritus deposited by Late Pleistocene ice sheets (Emery and Uchupi, 1984; Poppe at al., 2003), exhibit the largest variances found in our analysis (~3-10 ϕ^2). Most of these sample regions have average mean grain sizes > 2 ϕ, with the exception of < 50 m water depth regions both north and south of Cape Ann, MA and directly off Cape Cod. In these areas it is not uncommon for samples to alternate between fine grained muds or sands and coarser material, up to and including gravel. Along the U.S. Pacific shelf and Gulf of Mexico shelf, west of Florida, average mean grain sizes are generally ~2-5 ϕ, and variances are mostly between ~0.8 and 2.7 ϕ^2.

(3) Aside from the evident association of shorter decorrelation lengths along the Florida shelf, decorrelation lengths in general do not exhibit much in the way of regional continuity.

We utilize inter-parameter graphs (Figure 12) to explore the relationships between the different statistical parameters estimated from the usSEABED continental shelf sample regions. Figure 12a displays average mean grain size in each sample region plotted against field variance. At first examination, there appears to be no trend between the two parameters. However, the scatter in the plot is largely driven by the regions with the largest field variance values. These regions are localized in the Gulf of Maine and Florida shelf areas, where we have cause to presume that the enhanced variance is being driven by the presence of gravel or shell patches. If we remove all results from these two regions (Figure 12b), a clear positive correlation is observed between the average and field variance of the mean grain size in ϕ (which translates into an inverse correlation in mm), with separate correlations are noted for parsed and extracted data results (correlation coefficients are +0.74, with 99% confidence, and +0.66, with 99% confidence for extracted and parsed, respectively), with the parsed samples exhibiting larger variances and/or coarser grain sizes (lower ϕ values). Regression lines for both parsed extracted measurements are also plotted on Figure 12b (for parsed: $y = 0.157 + 0.586x$; for extracted: $y = -0.154 + 0.287x$).

Other inter-parameter graphs (decorrelation length vs. average mean grain size in Figure 12c; decorrelation length vs. mean grain size variance in Figure 12d; noise variance vs. average mean grain size in Figure 12e; and noise variance vs. mean grain size in Figure 12f) evince no clear correlations. We include here measurements of the noise variance plotted against the average and field variance. Earlier we noted an evident correlation between the noise variances derived by parsed and extracted records of mean grain size. There is no self-evident reason why such a correlation should exist. One possibility is that noise variance for each is somehow related to the physical parameters of the mean grain size field, so that both parsed and extracted noise variances are responding to a common input. The lack of correlations noted in Figures 12d and 12f does not support this supposition, at least as related to the correlated component of the field. We cannot, however, discount the possible existence of an uncorrelated component to the field, or at least a component which has a shorter decorrelation scale than can be measured by the by the available spatial density of samples. If such a component does exist, it would contribute to what we identify as the noise variance, both for extracted and parsed measurements, thereby inducing a correlation between the two.

5. Example application: mapping grain size character of the Long Island shelf

The Long Island shelf region exhibits complex sediment character and distribution due to several factors such as: proximity to terminal moraine glacial deposits that compose Long Island, underlying framework geology, and transgressive marine processes associated with approximately 100 m of Holocene sea level rise (Williams, et al., 2006a). In addition to providing basic information about the spatial variability of a field, the semivariogram characterization provides important constraints on the production of maps through interpolation of point data. Ordinary kriging is a well-known interpolation methodology that explicitly utilizes the semivariogram in a weighted averaging algorithm (e.g., Cressie, 1990; Deutsch and Journel, 1992). The primary advantage Kriging has over deterministic interpolation methods, such as splines (e.g., Smith and Wessel, 1990), is that it provides a geostatistical framework for estimating the error of the prediction. Other interpolation methods could be used, however, with similar results for map generation. The kriging solution can be identified as the expected value at an unsampled location given the data constraints at proximal and distal locations. We demonstrate kriging of the usSEABED mean grain size data on the Long Island shelf to 50 m water depth (Figure 13). This area includes two of our defined sample regions, from 0-20 m (area 5) and 20-50 m (area 11). The parsed and extracted semivariogram characterizations of the 0-20 m sample region are shown in Figure 8a. The 20-50 m semivariogram characterizations are nearly identical, allowing us to apply a single statistical characterization to the kriging interpolation of the combined area. Because the field variances and decorrelation lengths derived from both parsed and extracted records are very similar, we conclude that it is appropriate in this case to combine the two types of records for the interpolation with a simple static shift, a “bias-correction proxy”, to accommodate differences in the mean. Here that proxy is ~0.5 ϕ, which is the approximate difference between the average extracted and parsed mean grain sizes in these regions (Table 1). We subtracted this value from all of the extracted records under the assumption that the extracted values underreport coarse fraction. This is speculative, however, and other workers may consider other rationales for choosing how to apply the proxy. The resulting kriged field is shown in Figure 13a.

A direct interpolation of the usSEABED mean grain size records is not necessarily desirable, however. With a parsed record noise variance that is nearly double the field variance (Figure 8; Table 1), many positive and negative spikes appear in the mappings. Goff et al. (2006) recently formulated a methodology for resampling noisy, correlated data to mitigate the spikes prior to resampling. The method employs both a characterization of the field semivariogram (as characterized by the field variance, decorrelation distance and fractal dimension), and an *a priori* characterization of the data uncertainty. Here we assume that the data uncertainty is well-characterized by the square root of our estimation of the noise variance. Figure 13b displays the results of kriging the resampled mean grain size data, clearly demonstrating a significant reduction in the number and intensity of spikes.

For the Long Island shelf data set, the accuracy of the mean grain size map can be checked qualitatively by comparing it to existing USGS backscatter data collected off western Long Island, NY (Schwab et al. 2000). In Figure 14, we compare overlapping components of the two maps. Bearing in mind the much lower spatial resolution of the seafloor sample map (of order kilometers) as compared to the acoustic backscatter (of order meters), there are evident associations of coarser grain sizes on the mean grain size map to regions of higher backscatter intensity (i.e., sand shoals). This is particularly notable in the central part of the figure. A quantitative comparison between the two mapped values is presented in Figure 15. Considerable scatter is evident in this direct comparison, likely due both to the very different spatial resolutions of the two maps and to the generally erratic behavior of backscatter data (e.g., Goff et al., 2004). As noted previously, temporal variability of the usSEABED records may also contribute to spatial erraticity of the mean grain size values. The resampling algorithm mitigates these effects. The binned mean values (Figure 15), however, present a much clearer relationship. We first observe a general decrease in backscatter intensity with decreasing grain size going from very coarse sand (~-0.5 ϕ) to the medium/fine sand transition (~2 ϕ). This observation is consistent with what can be most readily observed qualitatively on Figure 14. At grain sizes finer than 2 ϕ, however, an inverted trend (increasing backscatter with decreasing grain size) is noted. A similar reversal in backscatter-versus-grain size trend, also occurring at fine-sand grain sizes, was noted by Goff et al. (2005; Figure 4)) within the Martha's Vineyard Coastal Observatory. We speculate that fine sands mark a transition between backscatter dominated by surface/grain size roughness and volumetric heterogeneity (e.g., Jackson et al., 1986). That is, at finer grain sizes, the acoustic energy is able to penetrate deeper into the sediments, and in so doing intersects with a greater cross-section of potential scatterers. Whether or not this is the case, however, the consistency of trends with another grain size-versus-backscatter study in a similar inner-shelf environment provides a measure of validation for our usSEABED-based mean grain size map of the Long Island shelf.

6. Conclusions and Discussion

In this paper, we have presented a methodology for statistical analysis of randomly-located, noisy point data, and applied it to the usSEABED records of mean grain size on the continental shelf seabed. The method has proven robust at obtaining estimates of the field variance and decorrelation distance, as well as estimates of the data noise variance. However, the erratic nature of semivariograms generated from such randomly-located data generally precludes robust estimation of the fractal dimension.

As primary component of the study we examined the suitability of the aggregated usSEABED data collection for mapping and variability analysis. Our deterministic and statistical comparison between the parsed and extracted forms of mean grain size data reveal some differences. As expected, the noise variance tends to be larger for the parsed records (by ~0.2-1.0 ϕ^2), which reflects a higher level of uncertainty in the measurements. Greater temporal variability (i.e., timing of sample collection) may also be important. At present, temporal information cannot be extracted from the usSEABED database, but it is likely that the word-based data records span a much greater range in dates. Any temporal effects on grain size measurements (e.g., changes in sedimentary conditions, changes in navigational resolution) will presumably factor into the data uncertainty. Higher levels of uncertainty in the parsed measurements might also be related to the likelihood that they are more likely to incorporate a wider set of materials, such as coarse biogenics.

In general, the extracted mean grain sizes tend to exhibit higher ϕ values (finer grain sizes), ~0.5 ϕ on average, and lower field variance relative to the parsed mean grain sizes. Both observations might be explained by a tendency for grain size analysts to discard the very coarsest fraction of a sediment, particularly if it contains shell material. These differences between parsed and extracted measurements are, however, somewhat regionally dependent, and it is not possible to formulate a precise universal conversion factor between the two. Nevertheless, if sufficient numbers of each type of data exist within a particular sample region, it should be possible to empirically define a local conversion so that the two types of data can be used together, along with their respective uncertainties, for quantitative applications such as mapping.

Our analysis of sample regions for the usSEABED records on the continental shelf reveal considerable geographic variability in the estimated parameters of field variance (Figure 10) and decorrelation distance (Figure 11). High field variances and short decorrelation lengths on the Florida shelves may indicate a high level of patchiness due to shelly material. Very high variances in the Gulf of Maine may be a result of residual glacio-fluvial gravel patches interspersed with fine-grained sediments. Elsewhere, we observe a fairly strong inverse relationship between the average mean grain size and the field variance (expressed as a positive correlation in ϕ units). We are uncertain as to the cause of this correlation.

Other than the small values on the Florida shelf, the estimated decorrelation length scales do not present coherent geographical relationships. Unlike the results of Jenkins and Goff (2007) for the analysis of mean grain size measurements in the Adriatic Sea, we do not find evidence on the U.S. Atlantic margin for any consistent depth relationship for this parameter (other regions were insufficiently sampled to discriminate sample regions based on water depth). We believe that analysis of more sample areas from a greater variety of settings will be needed to decipher the primary influences on decorrelation length scale. We suggest here that it may be controlled by competing relationships of geologic inputs (e.g., sediment facies), which probably tend toward larger decorrelation length scales, and oceanographic reworking, which probably tends toward shorter length scales (e.g., bedforms).

In Figure 9c we presented evidence that the noise variance estimated from parsed and extracted mean grain size measurements are correlated. Assuming the noise variance is related only to the data uncertainty, there is no reason to expect such a correlation, suggesting that noise is somehow influenced by the properties of the field. However, no such evidence could be found in our interparameter plots presented in Figures 12e and 12f. To explain these observations, we hypothesize that a very short-scale of field variability exists that is superimposed on the larger scale of variability that we discern through estimate of the decorrelation length of the semivariogram, and that the decorrelation length of this shorter scale variability is shorter than the resolution scale of the sample data. In other words, the portion of data variability that we identify as “noise” includes both a real field component and a data uncertainty component. If true, then we cannot directly distinguish between the two, although we may be able to infer the field component if we are able to postulate globally constant values of uncertainty for parsed and extracted measurements. More data analysis will be required to determine if that is the case.

Our example using the Long Island shelf data (Figures 13, 14) shows that usSEABED can reliably be utilized for creating maps of seafloor mean grain size and possibly other sediment characteristics. Due to the noisy character of the data, some sort of filtering or other noise reduction algorithm (e.g., Goff et al., 2006) is recommended prior to map generation. To combine the parsed and extracted measurements, a bias correction proxy must be applied, and such a correction should be evaluated individually for each region of interest. For the Long Island shelf data, a simple mean correction of 0.5 ϕ was found to be suitable because the semivariogram statistics were otherwise found to be very similar between the two types of data. Recognizing that coarse content is excluded from many analytic results, we applied the correction by subtracting it from the extracted data. Other regions, however, exhibit significant difference in both the mean and variance of parsed versus extracted mean grain size values, and in those cases a more complex bias correction proxy must be devised.

Acknowledgments. The authors thank the Office of Naval Research for support under grants N00014-05-1-0079 (JAG) and N00014-05-1-0080 (CJJ), and the USGS/Coastal and Marine Geology Program (SJW). We particularly wish to thank the many people and institutions who have contributed their data to usSEABED. We acknowledge important assistance with the usSEABED database by Matthew Arsenault, Jane A. Reid, Halimeda Kilbourne, Jamey Reid and Brian Buczkowski of the USGS. Helpful comments on an earlier draft were provided by Wayne Baldwin and Walter Barnhardt for an internal USGS review, and two anonymous journal reviewers. UTIG contribution #____.

References

Adler, R.J., 1981. The Geometry of Random Fields. John Wiley, New York, 280pp.

Atallah, L., Probert Smith, P.J., 2004. Automatic seabed classification by the analysis of sidescan sonar and bathymetric imagery. IEEE Proceedings on Radar and Sonar Navigation 151, 327-336.

Bartholomä, A., 2006. Acoustic bottom detection and seabed classification in the German Bight, southern North Sea. Geo-Marine Letters 26, 177-184.

Buczkowski, B.J., Reid, J.A., Jenkins, C.J., Reid, J.M., Williams, S.J., Flocks, J.G., 2006. usSEABED: Gulf of Mexico and Carribbean (Puerto Rico and U.S. Virgin Islands) Offshore Surficial Sediment Data Release. U.S. Geological Survey Data Series 146, version 1.0, Online at http://pubs.usgs.gov/ds/2006/146/.

Calder, B., 2006. On the uncertainty of archive hydrographic data sets. IEEE Journal of Ocean Engineering 31, 249-265.

Christakos, G., 1992. Random field models in Earth sciences. Academic Press Inc., San Diego, 474 pp.

Cressie, N., 1990. The origins of kriging. Mathematical Geololgy 22, 239-252.

Deutsch, C.V., Journel, A.G., 1992. GSLIB geostatistical software library and user’s Guide. Oxford University Press, New York, 340pp.

Emery, K.O., Uchupi, E., 1984. The Geology of the Atlantic Ocean. Springer-Verlag, New York, 1050pp.

Ferrini, V L., Flood, R.D., 2006. The effects of fine-scale surface roughness and grain size on 300 kHz multibeam backscatter intensity in sandy marine sedimentary environments. Marine Geology 228, 153-172.

Folk, R.L., 1974. The petrology of sedimentary rocks. Hemphill Publishing Co., Austin, Texas., 182pp.

Goff, J A., Jordan, T.H., 1988. Stochastic Modeling of Seafloor Morphology: Inversion of Sea Beam data for second-order statistics. Journal of Geophysical Research 93, 13,589-13,608.

Goff, J.A., Jordan, T.H., 1989. Stochastic Modeling of Seafloor Morphology: resolution of topographic parameters by Sea Beam data. IEEE Journal of Ocean Engineering 14, 326-337.

Goff, J. A., Holliger, K., Levander, A.R., 1994. Modal fields: A new method for characterization of random velocity heterogeneity. Geophysical Research Letters 21, 493-496.

Goff, J.A., Olson, H.C., Duncan, C.S., 2000 Correlation of sidescan backscatter intensity with grain-size distribution of shelf sediments, New Jersey margin. Geo-Marine Letters 20, 43-49.

Goff, J.A., Kraft, B.J., Mayer, L.A., Schock, S.G., Sommerfield, C.K., Olson, H.C., Gulick, S.P.S., Nordfjord, S., 2004. Seabed characterization on the New Jersey middle and outer shelf: Correlability and spatial variability of seafloor sediment properties. Marine Geology 209, 147-172.

Goff, J.A., Mayer, L.A., Traykovski, P., Buyenevich, I., Wilkins, R., Raymond, R., Glang, G., Evans, R.L., Olson, H., Jenkins, C., 2005. Detailed investigation of sorted bedforms, or “rippled scour depressions,” within the Martha’s Vineyard Coastal Observatory, Massachusetts. Continental Shelf Research 25, 461-484.

Goff, J.A., Jenkins, C., Calder, B., 2006. Maximum likelihood resampling of noisy, spatially correlated data. Geochemistry, Geophysics and Geosystems 7, doi:10.1029/2006GC001297.

Grune, D., Jacobs, C.J.H., 1990. Parsing Techniques - A Practical Guide. Ellis Horwood, Chichester, England, 320pp.

Hamilton, E.L., Bachman, R.T., 1982. Sound velocity and related properties in marine sediments. Journal of the Acoustical Society of America 72, 1891-1904.

Harris, C.K., Butman, B., Traykovski, P., 2003. Winter-time circulation and sediment transport in the Hudson Shelf Valley. Continental Shelf Research 23, 801-820.

Inman, D.L., 1952. Measures for describing the size distribution of sediments. Journal of Sedimentary Petrology 22, 125–145.

Jackson, D.R., Winebrenner, D.P., Ishimaru, A., 1986. Application of the composite roughness model to high frequency bottom scattering. Journal of the Acoustical Society of America 79, 1410-1422.

Jakobsson, M., B. Calder, Mayer, L., 2002. On the effects of random errors in gridded bathymetric compilations. Journal of Geophysical Research 107, doi:10.1029/2001JB000616.

Jenkins, C.J. 1997. Building offshore soils databases. Sea Technology 38, 25-28.

Jenkins, C.J. 2002. Automated digital mapping of sediment colour descriptions. Geo-Marine Letters 22, 181-187.

Jenkins, C.J., Goff, J.A., submitted. Competent interpolation for seabed substrates, with uncertainty calculations. Continental Shelf Research.

Jones, M.B., Schildhauer, M.P., Reichman, O.J., Bowers, S. 2006. The New Bioinformatics: Integrating Ecological Data from the Gene to the Biosphere. Annual Review of Ecology, Evolution, and Systematics 7, 519-544.

Kerr, J.T., Southwood, T.R.E., Cihlar, J., 2001. Remotely sensed habitat diversity predicts butterfly species richness and community similarity in Canada. Proceedings of the National Academy of Sciences 98, 11,365-11,370

Lapinski, A-L.S., Chapman, D.M.F., 2005. The effects of ignored seabed variability in geoacoustic inversion. Journal of the Acoustical Society of America 117, 3524-3538.

Menke, W., 1989. Geophysical Data Analysis: Discrete Inverse Theory, Revised Edition. Academic Press, New York, 289pp.

Moore, J., Gutierrez , E.G., Mecray , E.L., ten Brink , M.R B., 2002. Methods. In: Physical Properties of Long Island Sound Sediment Cores. U.S. Geological Survey Open-File Report 02-372. Online at: http://pubs.usgs.gov/of/2002/of02-372/methods.htm.

NOAA, 2007. Coastal Relief Model. National Geophysical Data Center, Boulder, CO, USA. CD-ROM. Online at “http://www.ngdc.noaa.gov/mgg/coastal/coastal.html”.

Ogushwitz, P.R., 1985. Applicability of the Biot theory. II. Suspensions. Journal of the Acoustical Society of America 77, 441-452.

Osenberg, C.W., Sarnelle, O., Goldberg, D.E., 1999. Meta-Analysis in Ecology: Concepts, Statistics, and Applications. Ecology 80(4), 1103-1104.

Ormsby, T., Napoleon, E., Burke, R., Groessl, C., Feaster, L., 2001. Getting to know ArcGIS Desktop. ESRI Press, Redlands, California, 552pp.

Poppe, L.J., Eliason, A.H., Fredericks, J.J., Rendigs, R.R., Blackwood D., Polloni, C.F., 2001. USGS East-coast sediment analysis: Procedures, database and georeferenced displays, U.S. Geological Survey Open File Report 00-358. On line at "http://pubs.usgs.gov/of/2000/of00-358/text/contents.htm."

Poppe, L.J., Paskevich, V.F., Williams, S.J., Hastings, M.E., Kelly, J.T., Belknap, D.F., Ward, L.G., FitzGerald, D.M., Larsen, P.F., 2003. Surficial sediment data from the Gulf of Maine, Georges Bank and vicinity: a GIS compilation. U.S. Geological Survey Open-file Report 03-001, CD-ROM. Online at "http://pubs.usgs.gov/of/2003/of03-001/".

Poppe, L.J., Williams, S.J., Paskevich, V.F., Eds., 2005. USGS East-coast sediment analysis: procedures, database, and GIS data. U.S. Geological Survey Open-File Report 2005-1001, DVD-ROM. Online at: "http://woodshole.er.usgs.gov/openfile/of2005-1001/".

Pratson, L.F., Edwards, M. H., 1996. Introduction to advances in seafloor mapping using sidescan sonar and multibeam bathymetry. Marine Geophysical Research 18, 601-605.

Reid, J.M., Reid, J.A., Jenkins, C.J., Hastings, M.E., Williams, S.J., Poppe, L.J, 2005. usSEABED: Atlantic coast offshore surficial sediment data release. U.S. Geological Survey Data Series 118, version 1.0. Online at http://pubs.usgs.gov/ds/2005/118/.

Reid, J.A., Reid, J.M., Jenkins, C.J., Zimmermann, M., Williams, S.J., Field, M.E., 2006. usSEABED: Pacific Coast (California, Oregon, Washington) Offshore Surficial-Sediment Data Release: U.S. Geological Survey Data Series 182, version 1.0. Available online at http://pubs.usgs.gov/ds/2006/182.

Reineck, H.E., Singh, I.B., 1980. Depositional Sedimentary Environments with References to Terrigenous Clastics: 2d ed. Springer-Verlag, New York, 549 pp.

Schwab, W.C., Thieler, E.R., Allen, J.R., Foster, D.S., Swift, B.A., Denny, J.F., 2000. Influence of inner-continental shelf geologic framework on the evolution and behavior of the barrier-island system between Fire Island Inlet and Shinnecock Inlet, Long Island, New York. Journal of Coastal Research 16, 2, 408-422.

Smith, K.R., McConnaughey, R.A. 1999. Surficial sediments of the eastern Bering Sea continental shelf: EBSSED database documentation. U.S. Dep. Commer., NOAA Tech. Memo. NMFS-AFSC-104, 41p.

Smith, W. H. F., Wessel, P., 1990. Gridding with continuous curvature splines in tension. Geophysics 55, 293-305.

Stoll, R.D., 1977. Acoustic waves in ocean sediments. Geophysics 42, 715-725.

Vincent, C.E., Swift, D.J.P., Hillard, B., 1981. Sediment transport in the New York bight, North American Atlantic shelf. Marine Geology 42, 369-398.

Wessel, P., W H.F. Smith, 1998. New, improved version of the Generic Mapping Tools released. EOS Transactions of AGU 79, 579.

Williams, S. J., Jenkins, C., Currence, J., Penland, S., Reid, J., Flocks, J., Kindinger, J., Poppe, L., Kulp, M., Manheim, F., Hampton, M., Polloni, C., Rowland, J., 2003. New digital geological maps of U.S. continental margins: insights to sea floor sedimentary character, aggregate resources and processes. Proceedings of the International Conference on Coastal Sediments 2003, Corpus Christi, Texas, World Scientific Publishing Corporation and East Meets West Productions, Corpus Christi, Tex., 11 p., CD-ROM.

Williams, S.J., Arsenault, M.A., Poppe, L.J., Reid, J.A., Reid, J.M., Jenkins, C.J., 2006a. Surficial sediment character of the New York-New Jersey offshore continental shelf region; a

GIS compilation: U.S. Geological Survey Open-File Report 2006-1046. Online at http://pubs.usgs.gov/of/2006/1046.

Williams, S.J., Reid, J.A., Arsenault, M.A., Jenkins, C., 2006b. Characterization of sedimentary deposits using usSEABED for large-scale mapping, modeling and research of U.S. continental margins. Eos Transactions of AGU 87, Fall Meeting Supplement, Abstract H33B-1505.

Zadeh, L.A., 1965. Fuzzy Sets. Information and Control 8, 338-353.

Figure Captions

Figure 1. Location map of current (2007) usSEABED data coverage (250,000 records), color coded by mean grain size (Williams, et al., 2006b).

Figure 2. Conformance test between various measures of grain size: median, mode, Inman graphical mean, and moment mean. Moment mean grain size (1:1 line) is the accepted standard. The others deviate to a degree which may be compensated for in the processing of the analytical data. Based on 3813 samples from USGS laboratories (Reid, et al., 2005; Poppe et al., 2005).

Figure 3. Example calibration of parsed and extracted mean grain size using samples where both are available. The statistics are based on 10,029 sediment samples in the usSEABED database.

Figure 4. Location of usSEABED records within the mid-Atlantic Bight, color coded by mean grain size, and overlain on bathymetric contours (meters). Sample areas defined for this region are indicated by green polygons with yellow boarders.

Figure 5. Sample areas defined over the entire usSEABED database, color coded by the average of the parsed mean grain size measurements within the sample area. Numbered identifications provide reference for Table 1 statistical parameters.

Figure 6. A binned semivariogram (solid) derived from parsed mean grain size measurements in the 0-20 m depth range of the New York Bight (Figure 4). The best-fit von Kármán model with

noise spike is overlain (dashed), with parameter values as indicated. The fractal dimension of the model is 1.5, which corresponds to an exponential curve.

Figure 7. Plot of mean grain size estimated via extracted versus parsed methods, where samples of each type are separated by less than 200 m. Binned averages are also shown, both for extracted and parsed bins.

Figure 8. Semivariograms derived from both extracted and parsed mean grain size measurements within three sample areas: (a) the New York Bight, 0-20 m; (b) the Gulf of the Farallons, CA 0-150 m; and (c) Gulf of Maine just north of Cape Ann, 50-100 m. Area numbers refer to identifications in Figure 5. Best fit von Kármán models are overlain in dashed lines, with parameters as indicated.

Figure 9. Plots of extracted versus parsed statistical parameters from sample areas with adequate coverage of both types of data records. Dashed line indicates 1:1 correspondence. Circled symbols in (b) and (c) are from Gulf of Maine sample regions, and are discussed in the text. Correlation coefficients (ρ) are given for each plot, neglecting the outliers identified in (b) and (c).

Figure 10. Sample areas color coded by estimated field variance of mean grain size measurements. In regions where both extracted and parsed estimates are made, the maximum value is displayed. Numbered identifications provide reference for Table 1 statistical parameters.

Figure 11. Sample areas color coded by estimated decorrelation distance of mean grain size measurements. In regions where both extracted and parsed estimates are made, the average value, weighted by the number of samples of each, is displayed. Numbered identifications provide reference for Table 1 statistical parameters.

Figure 12. Interparameter plots of statistical parameters estimated from usSEABED mean grain size measurements. Sample areas are coded by parsed (PRS) or extracted (EXT), and by shelf region (ATL = Atlantic; GMX = Gulf of Mexico; PAC = Pacific). The data points in (b) are reproduced from those in (a), but without the values from the Gulf of Maine and the Florida shelf. These samples typically display very high variances, probably in association with the presence of gravel or shell patchiness. The remainder exhibit a clear trend, both for parsed and extracted measurements, which are illustrated with the dashed lines. Trends are otherwise not evident in the other interparameter plots displayed.

Figure 13. (a) Kriging interpolation of the usSEABED mean grain size data off the Long Island shelf to 50 m water depth. The statistical parameters noted on Figure 6 were utilized in the kriging operator. (b) Same as (a) for the mean grain size data after “resampling” according to the maximum a posteriori method of Goff et al. (2006), which decreases spiky artifacts. Dots indicate location of data records.

Figure 14. Comparison of overlapping portions of USGS acoustic backscatter data (a; from Schwab et al., 2000) and the interpolated, resampled mean grain size off the western Long Island shelf (b; from Figure 13b). Lighter shades indicate in (a) higher backscatter and coarser

sediment, darker shades indicate lower backscatter and finer sediments. Bathymetric contours on both plots, from the NOAA (2007) coastal relief model, are in meters.

Figure 15. Comparison of coregistered values (black dots) for backscatter intensity (Figure 14a) and interpolated mean grain size (Figure 14b). Backscatter values, originally gridded at 4 m, are averaged within 0.00167-degree cells (approximately 200 m). Cyan diamonds indicate average backscatter values within 0.25-ϕ grain size bins.

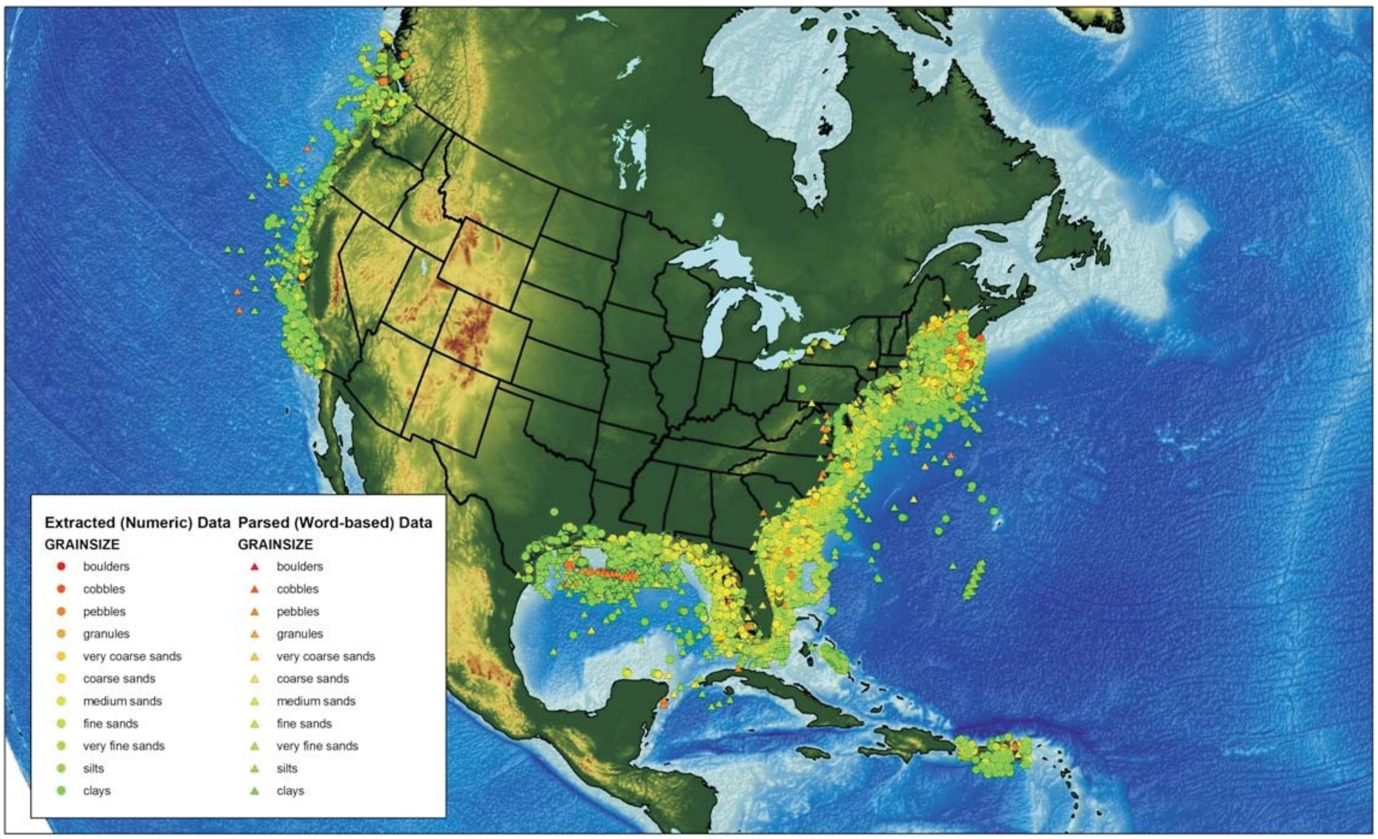

Extracted (Numeric) Data
GRAINSIZE
boulders
cobbles
pebbles
granules
very coarse sands
coarse sands
medium sands
fine sands
very fine sands
silts
clays
Parsed (Word-based) Data
GRAINSIZE
boulders
cobbles
pebbles
granules
very coarse sands
coarse sands
medium sands
fine sands
very fine sands
silts
clays

Figure 1

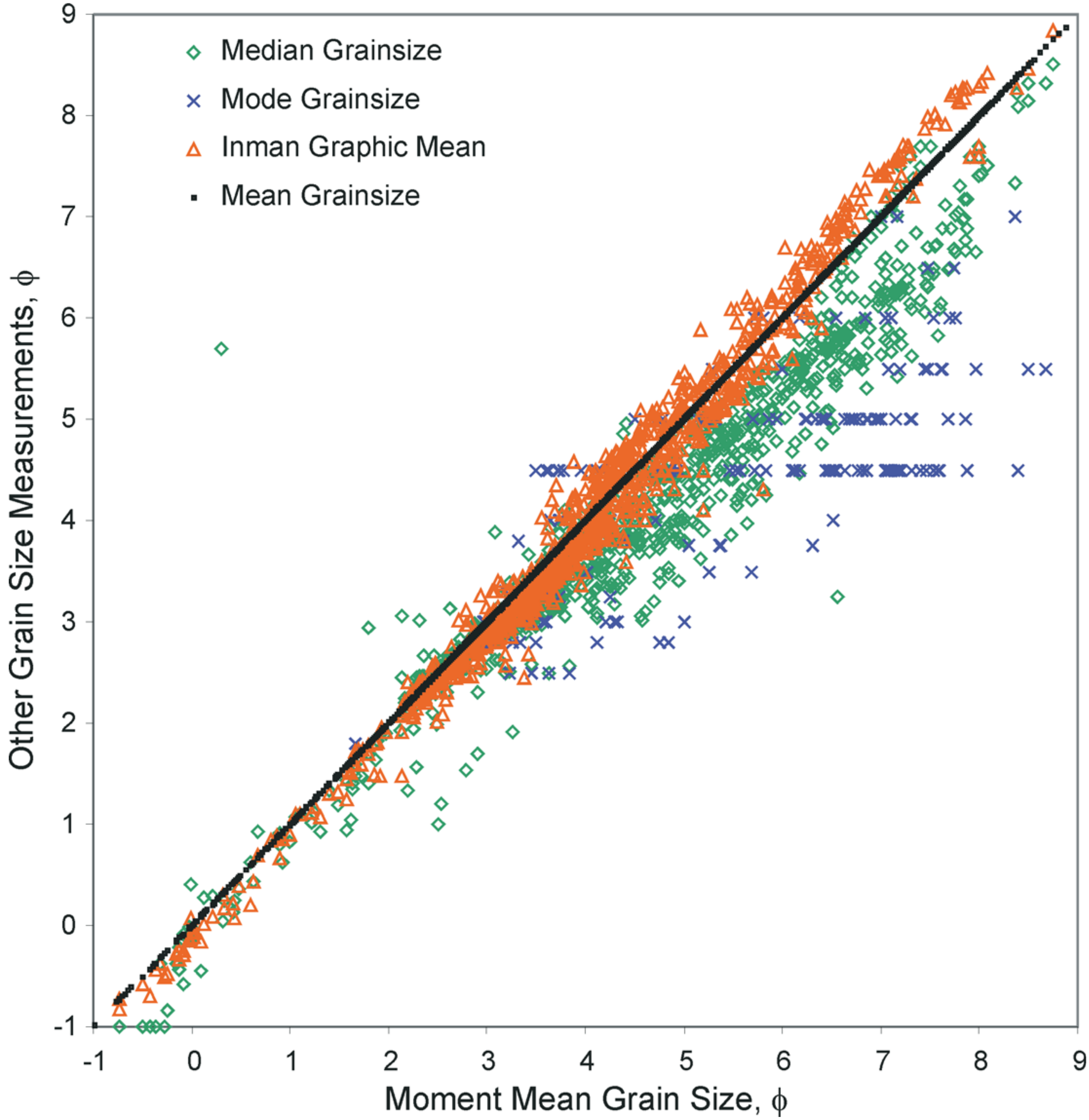
Median Grainsize
Mode Grainsize
Inman Graphic Mean
Mean Grainsize
Other Grain Size Measurements, ϕ
Moment Mean Grain Size, ϕ
9
8
7
6
5
4
3
2
1
0
-1
-1
0
1
2
3
4
5
6
7
8
9

Figure 2

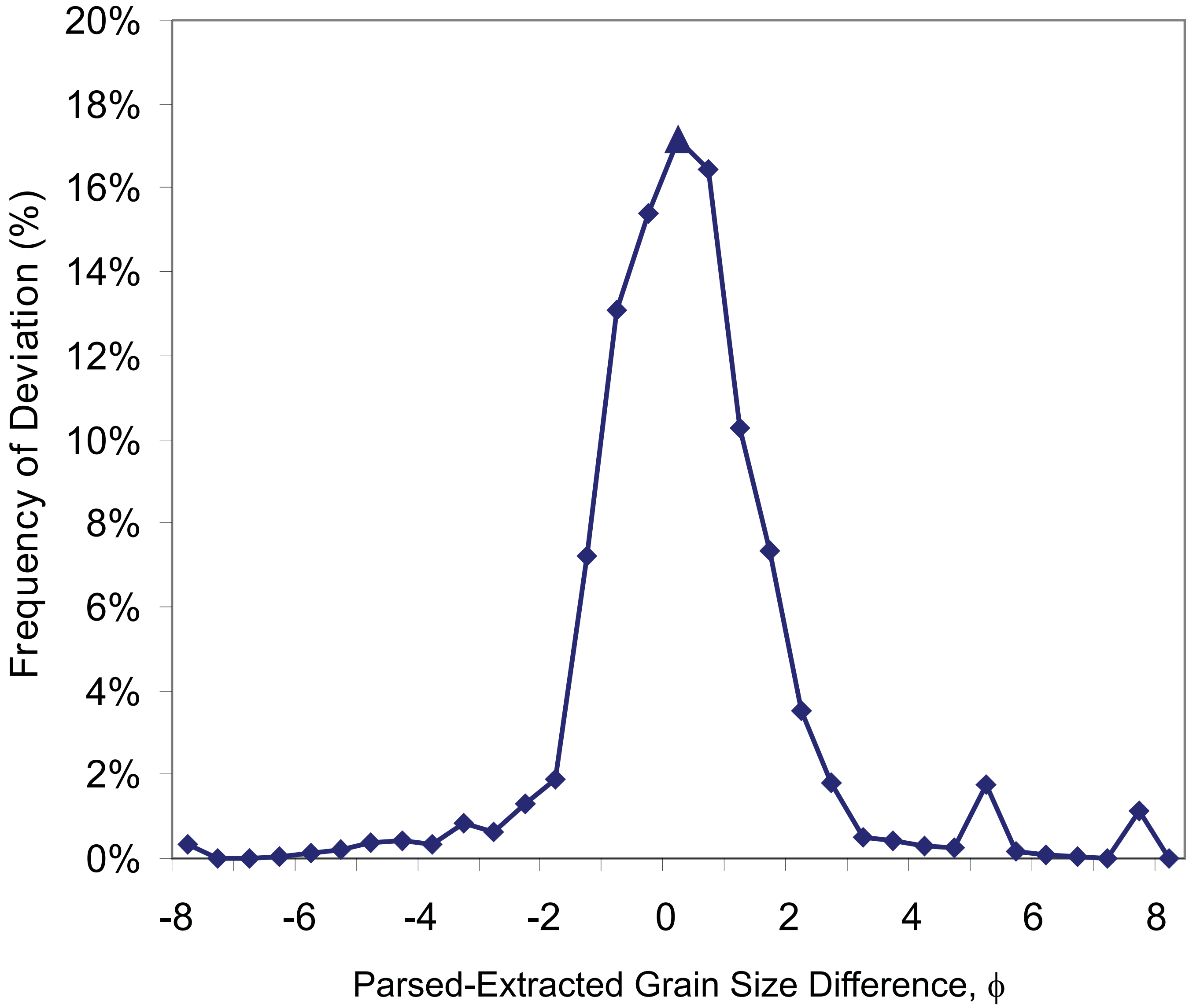
20%
18%
16%
14%
12%
10%
8%
6%
4%
2%
0%
Frequency of Deviation (%)
-8
-6
-4
-2
0
2
4
6
8
Parsed-Extracted Grain Size Difference, ϕ

Figure 3

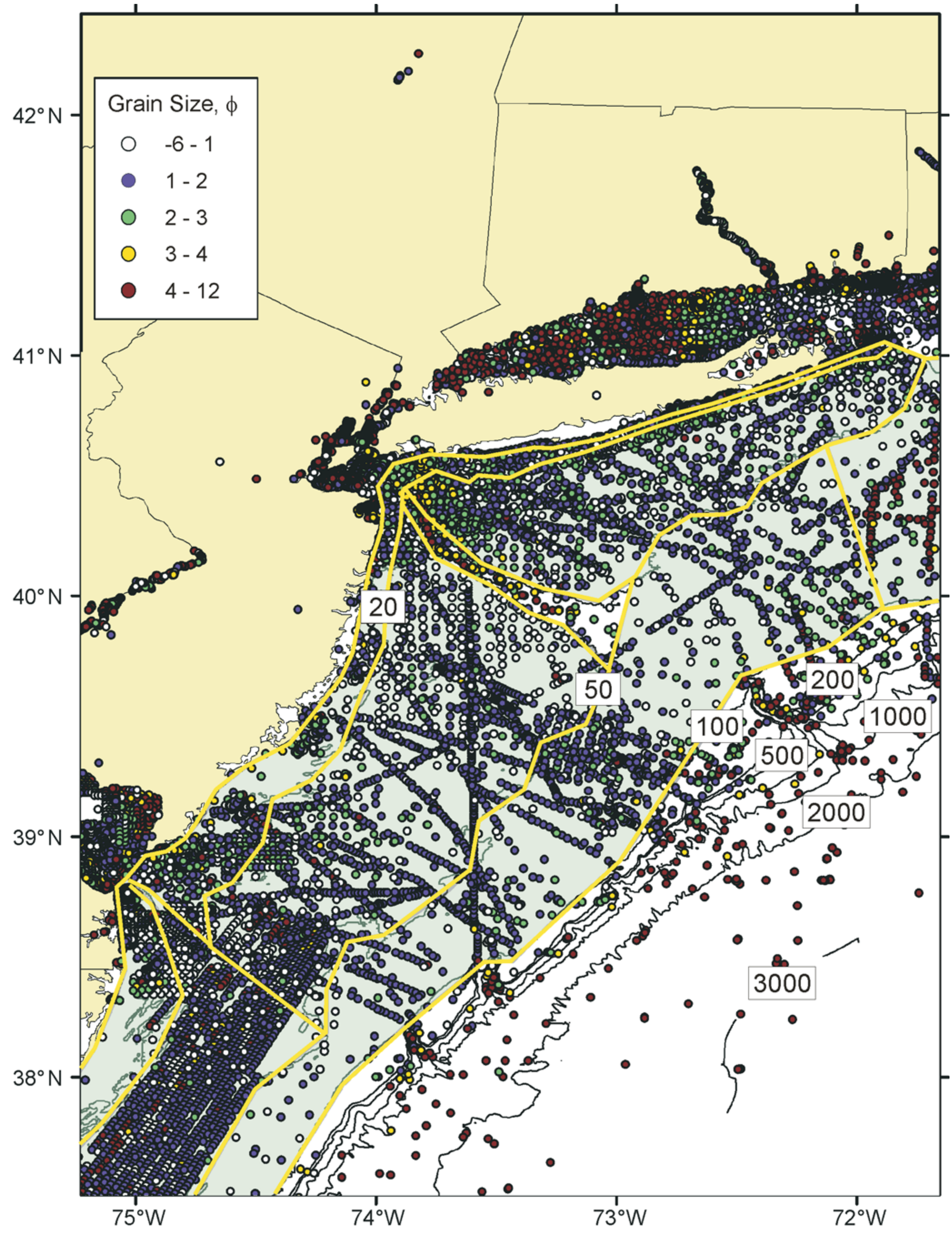

Grain Size, ϕ
-6 - 1
1 - 2
2 - 3
3 - 4
4 - 12
42° N
41° N
40° N
39° N
38° N
75°W
74°W
73°W
72°W
20
50
100
200
500
1000
2000
3000

Figure 4

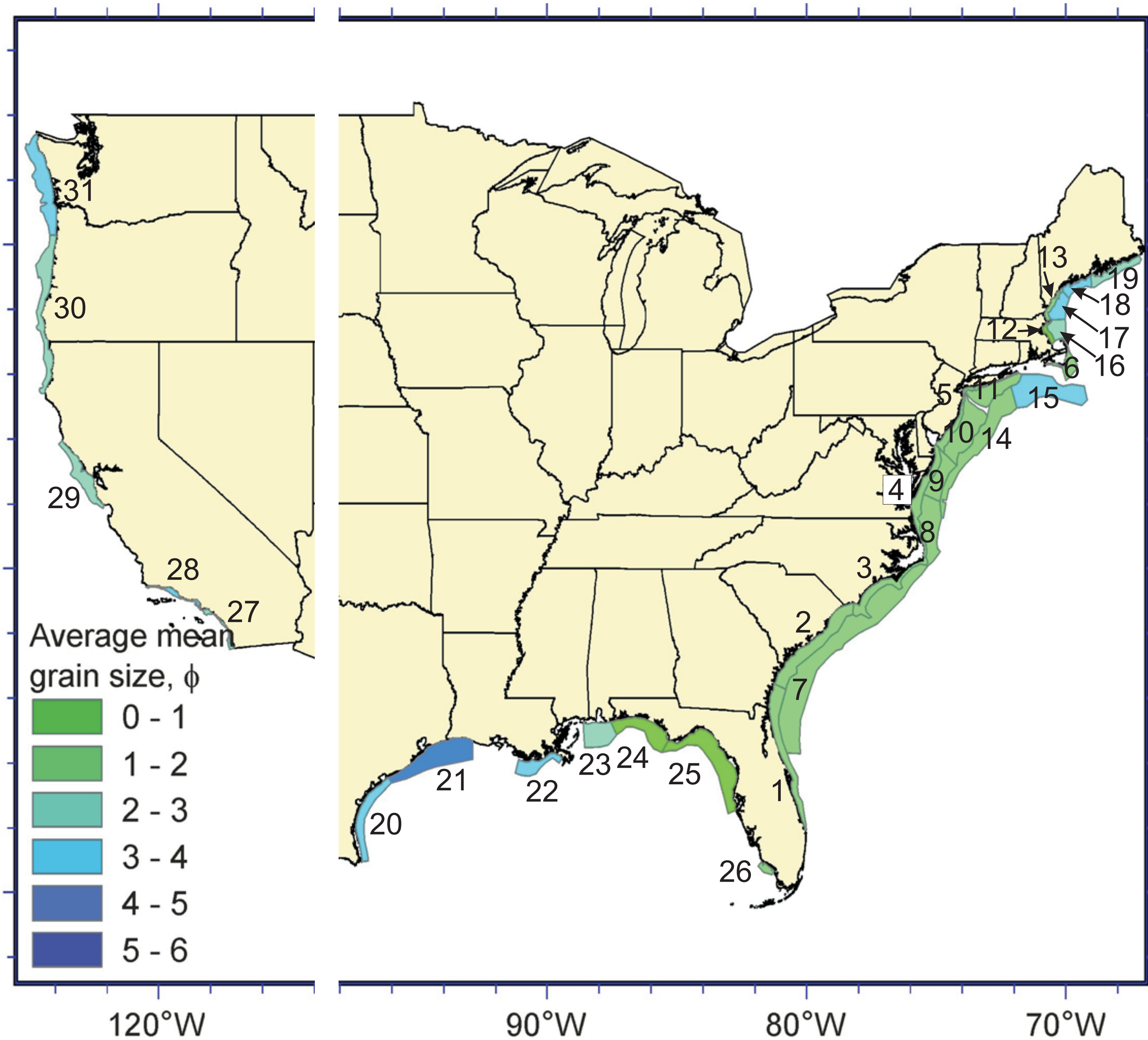
45°N
35°N
25°N
120°W
90°W
80°W
70°W
Average mean grain size, ϕ
0 - 1
1 - 2
2 - 3
3 - 4
4 - 5
5 - 6
1
2
3
4
5
6
7
8
9
10
11
12
13
14
15
16
17
18
19
20
21
22
23
24
25
26
27
28
29
30
31

Figure 5

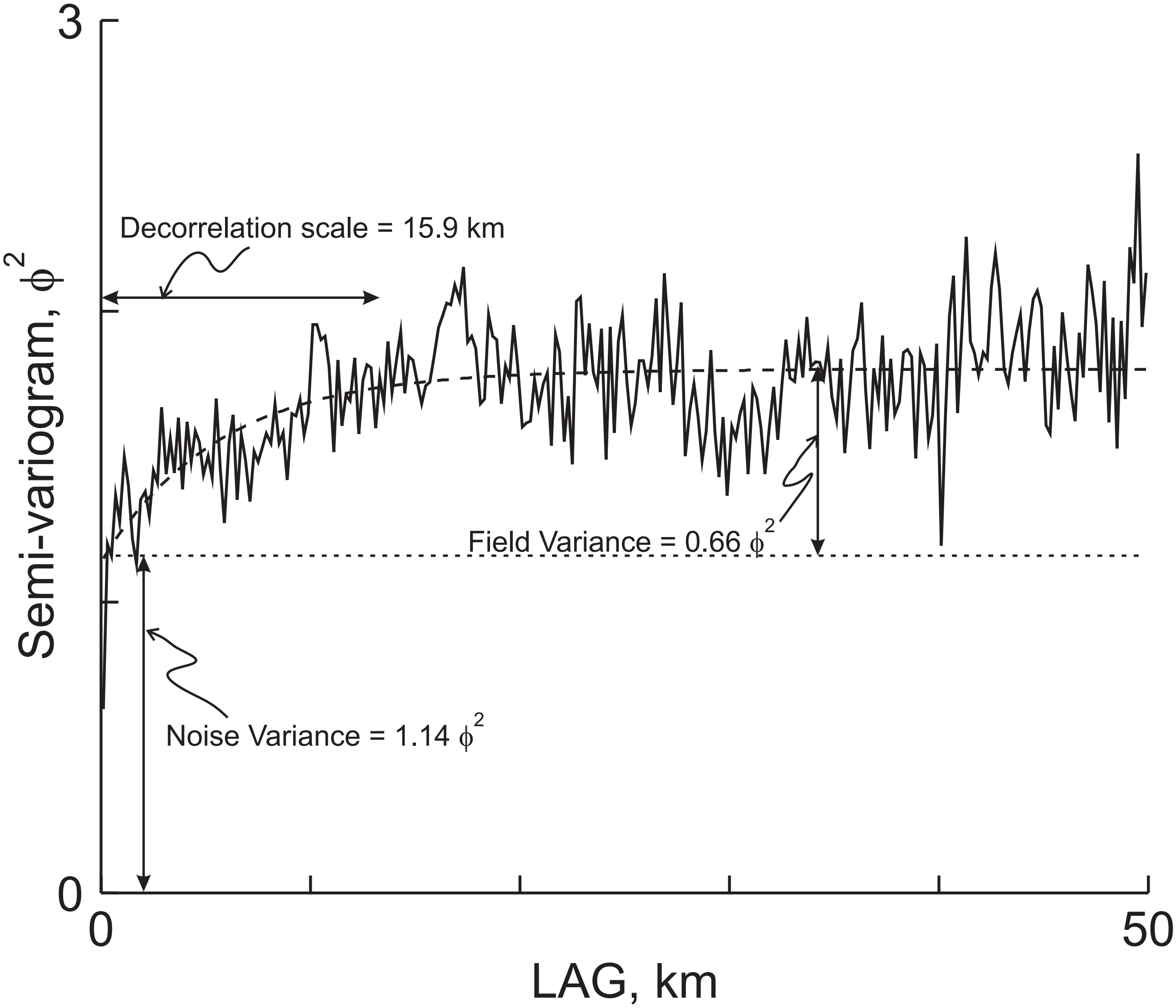
3
Semi-variogram, ϕ^2
Decorrelation scale = 15.9 km
Field Variance = 0.66 ϕ^2
Noise Variance = 1.14 ϕ^2
0
0
50
LAG, km

Figure 6

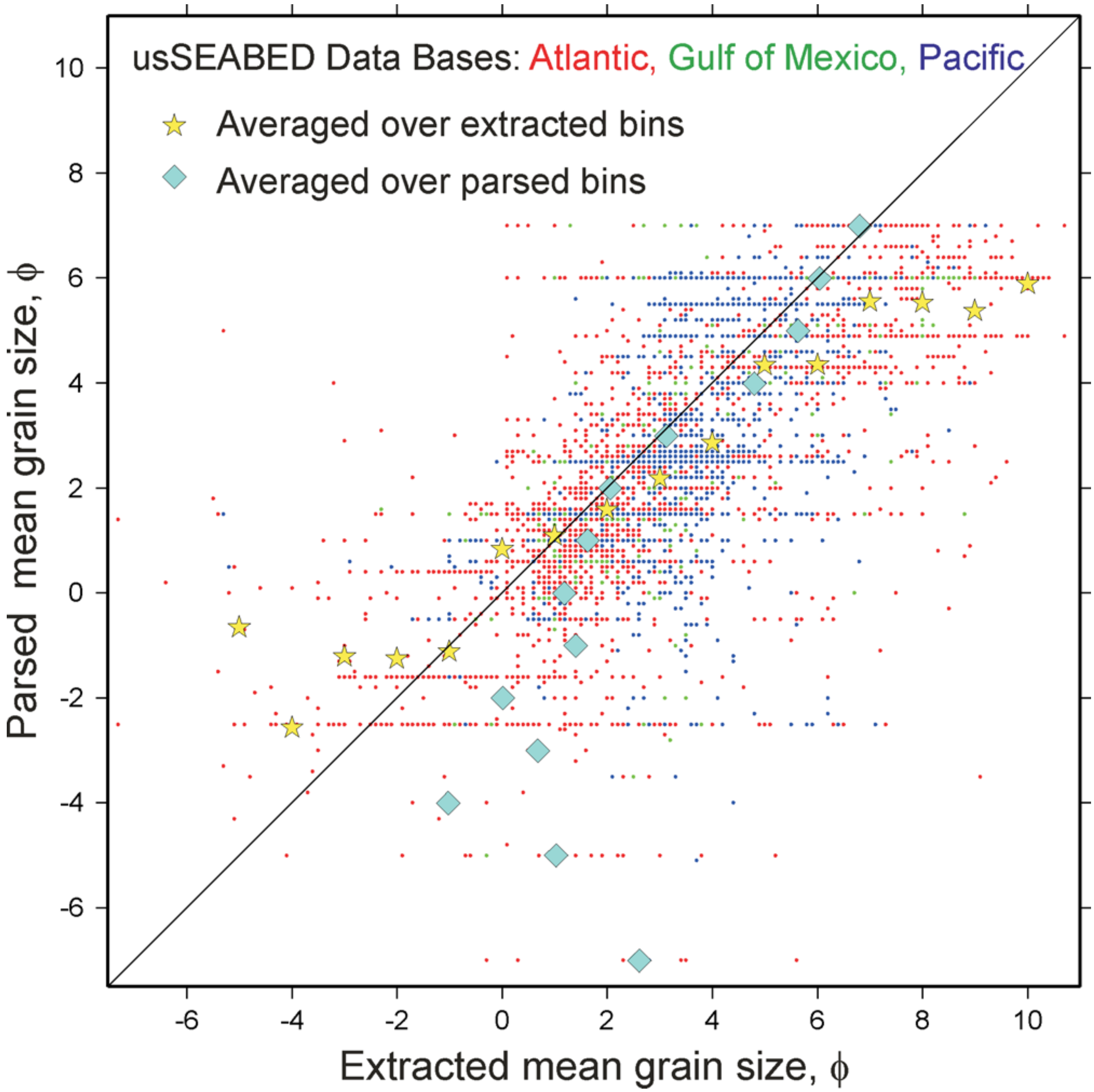
usSEABED Data Bases: Atlantic, Gulf of Mexico, Pacific
Averaged over extracted bins
Averaged over parsed bins
Parsed mean grain size, ϕ
Extracted mean grain size, ϕ
10
8
6
4
2
0
-2
-4
-6
-6
-4
-2
0
2
4
6
8
10

Figure 7

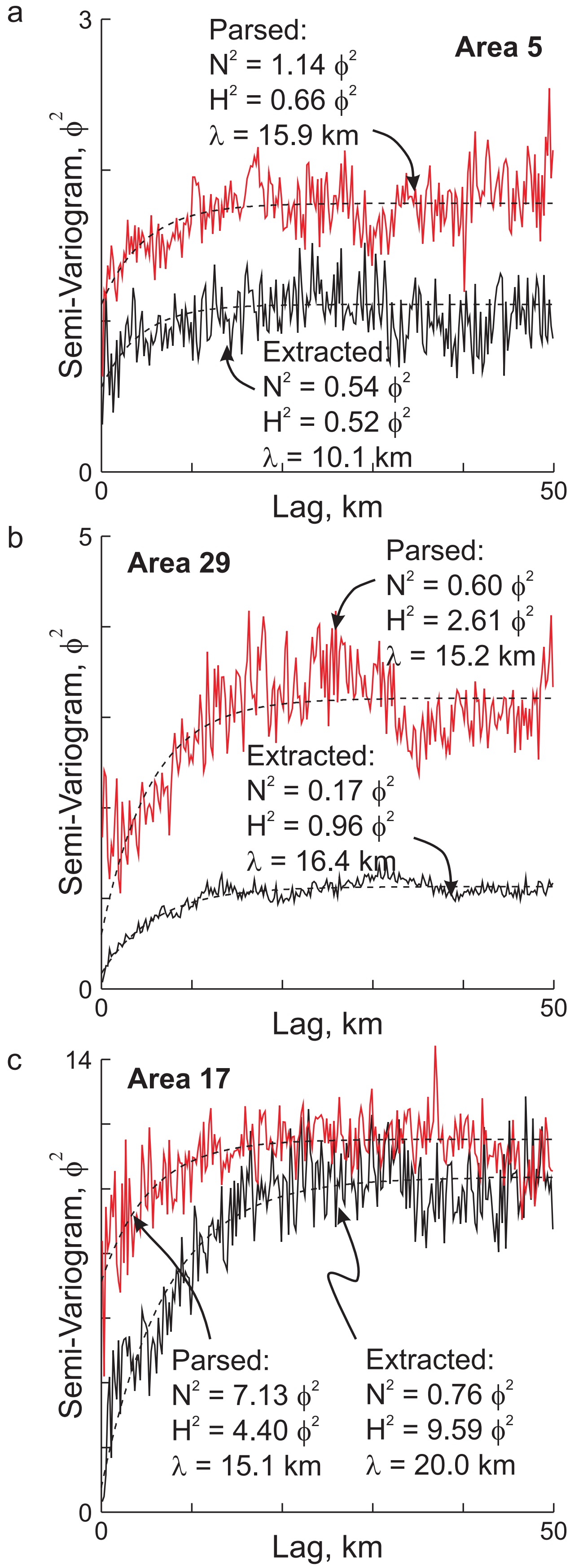
a
Area 5
Parsed:
N² = 1.14 ϕ²
H² = 0.66 ϕ²
λ = 15.9 km
Extracted:
N² = 0.54 ϕ²
H² = 0.52 ϕ²
λ = 10.1 km
Semi-Variogram, ϕ²
Lag, km
3
0
50
b
Area 29
Parsed:
N² = 0.60 ϕ²
H² = 2.61 ϕ²
λ = 15.2 km
Extracted:
N² = 0.17 ϕ²
H² = 0.96 ϕ²
λ = 16.4 km
Semi-Variogram, ϕ²
Lag, km
5
0
50
c
Area 17
Parsed:
N² = 7.13 ϕ²
H² = 4.40 ϕ²
λ = 15.1 km
Extracted:
N² = 0.76 ϕ²
H² = 9.59 ϕ²
λ = 20.0 km
Semi-Variogram, ϕ²
Lag, km
14
0
50

Figure 8

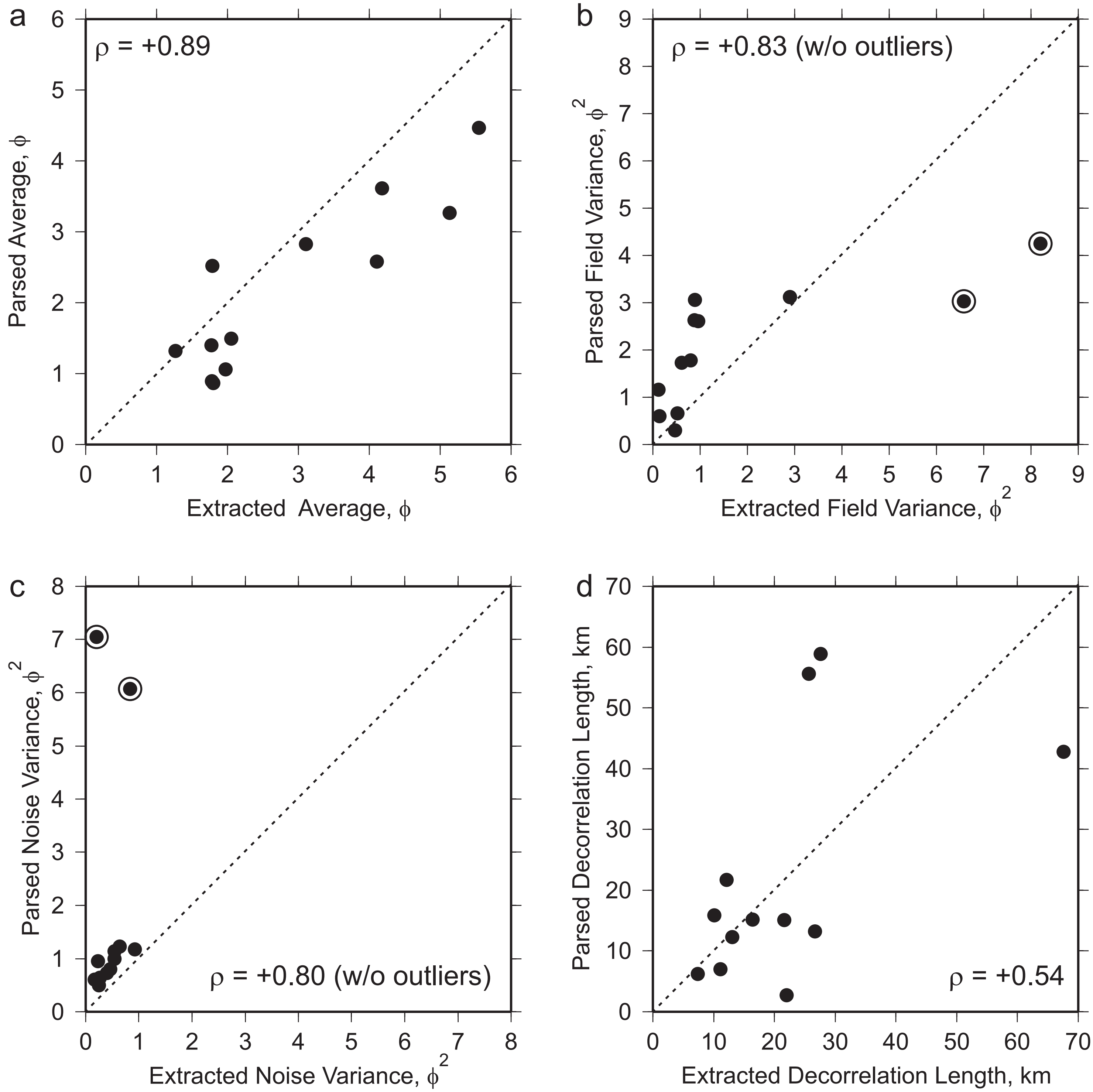
a
ρ = +0.89
Parsed Average, ϕ
Extracted Average, ϕ
b
ρ = +0.83 (w/o outliers)
Parsed Field Variance, ϕ2
Extracted Field Variance, ϕ2
c
ρ = +0.80 (w/o outliers)
Parsed Noise Variance, ϕ2
Extracted Noise Variance, ϕ2
d
ρ = +0.54
Parsed Decorrelation Length, km
Extracted Decorrelation Length, km

Figure 9

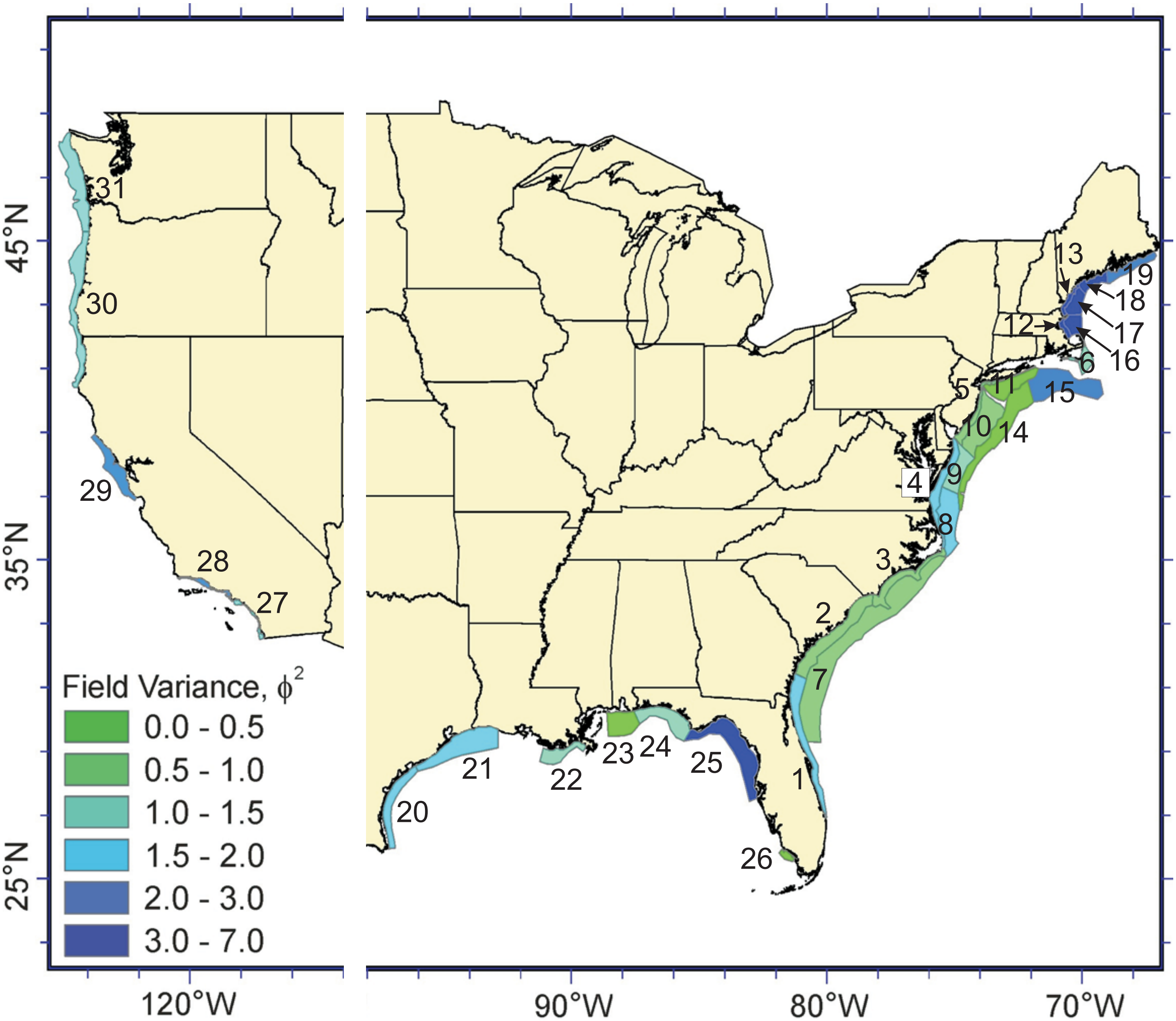

45°N
35°N
25°N
120°W
90°W
80°W
70°W
Field Variance, ϕ^2
0.0 - 0.5
0.5 - 1.0
1.0 - 1.5
1.5 - 2.0
2.0 - 3.0
3.0 - 7.0
1
2
3
4
5
6
7
8
9
10
11
12
13
14
15
16
17
18
19
20
21
22
23
24
25
26
27
28
29
30
31

Figure 10

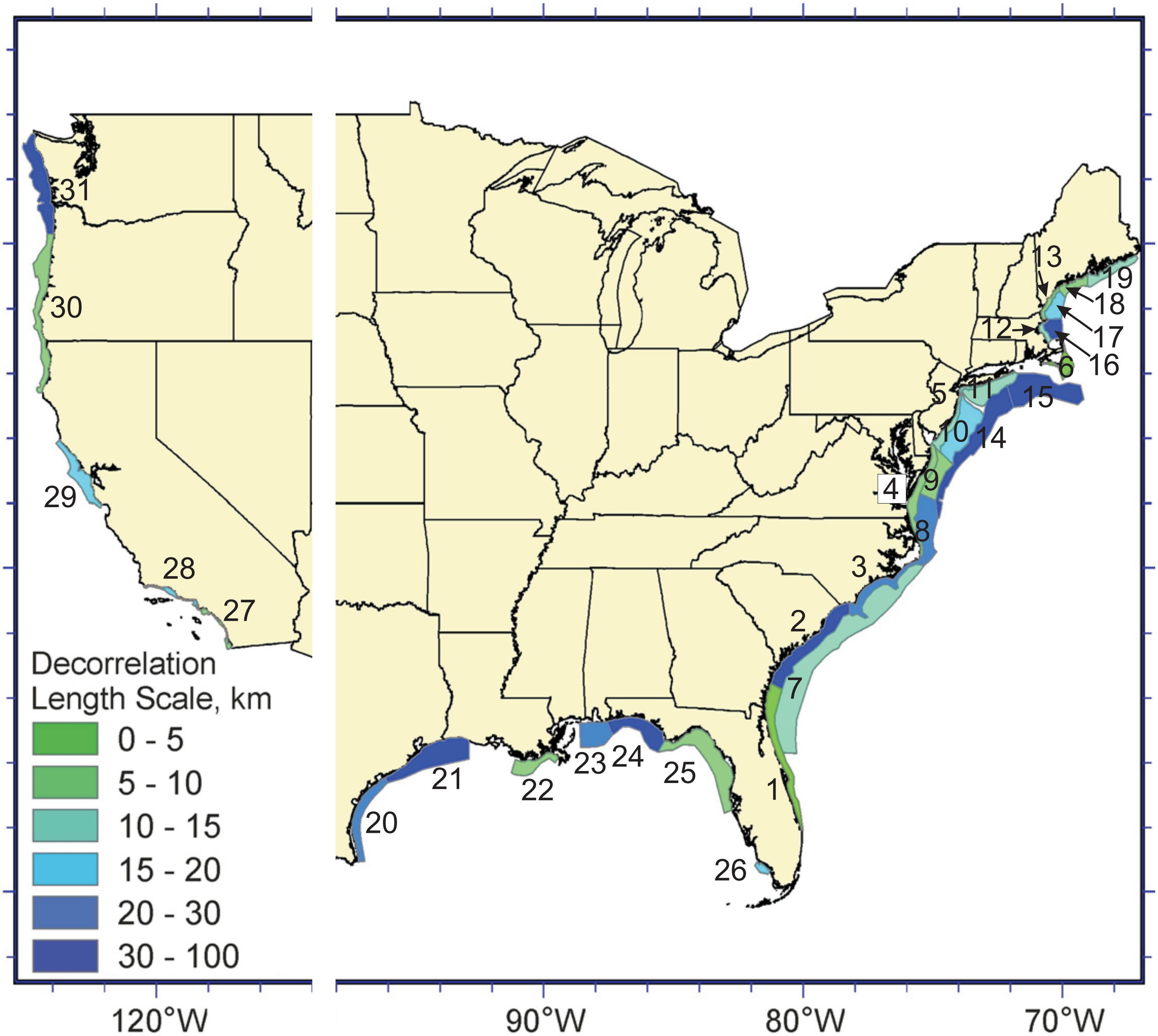

45°N
35°N
25°N
120°W
90°W
80°W
70°W
31
30
29
28
27
20
21
22
23
24
25
26
1
2
3
4
5
6
7
8
9
10
11
12
13
14
15
16
17
18
19
Decorrelation
Length Scale, km
0 - 5
5 - 10
10 - 15
15 - 20
20 - 30
30 - 100

Figure 11

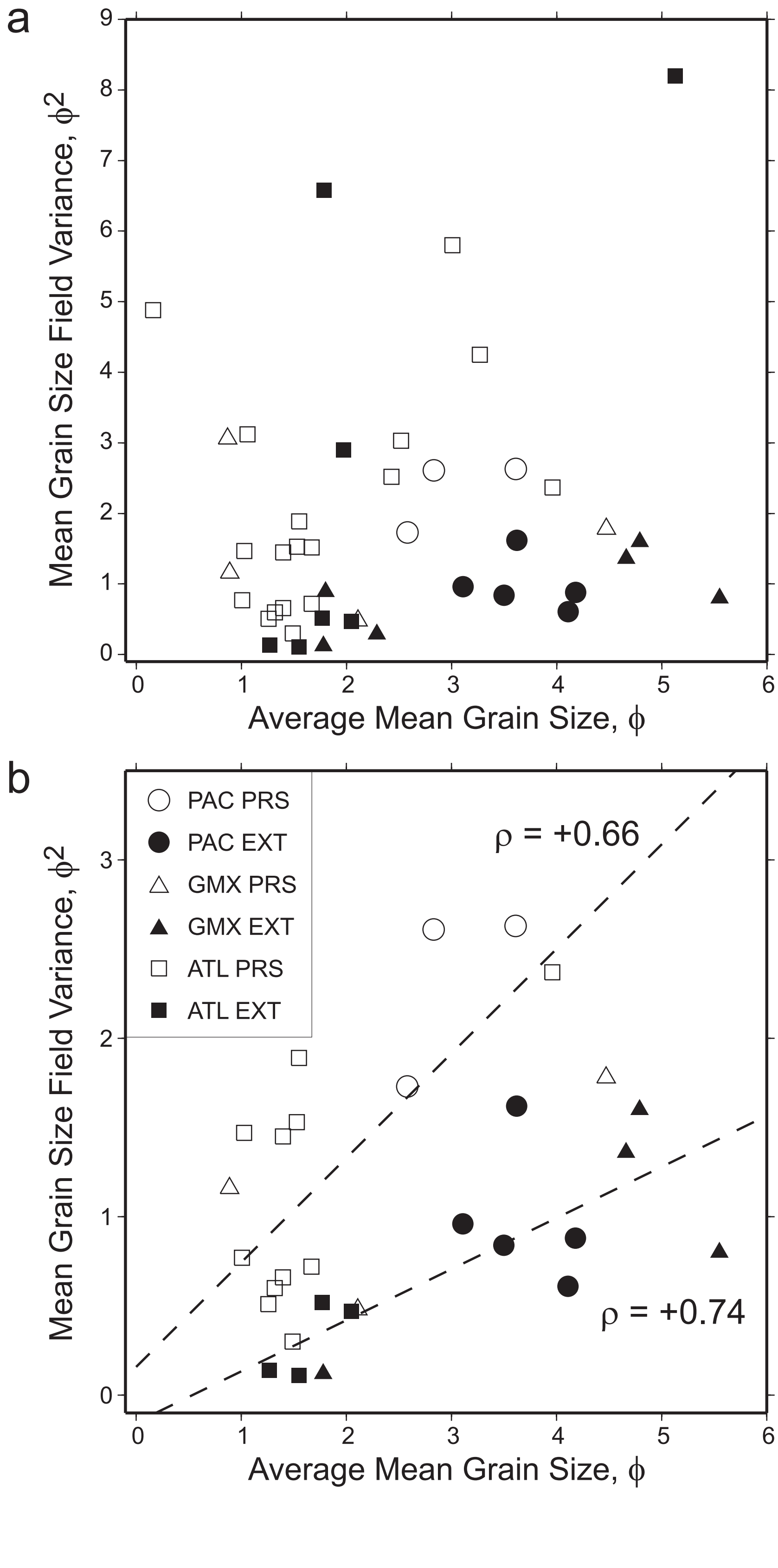

a
Mean Grain Size Field Variance, ϕ^2
Average Mean Grain Size, ϕ
b
PAC PRS
PAC EXT
GMX PRS
GMX EXT
ATL PRS
ATL EXT
ρ = +0.66
ρ = +0.74

Figure 12

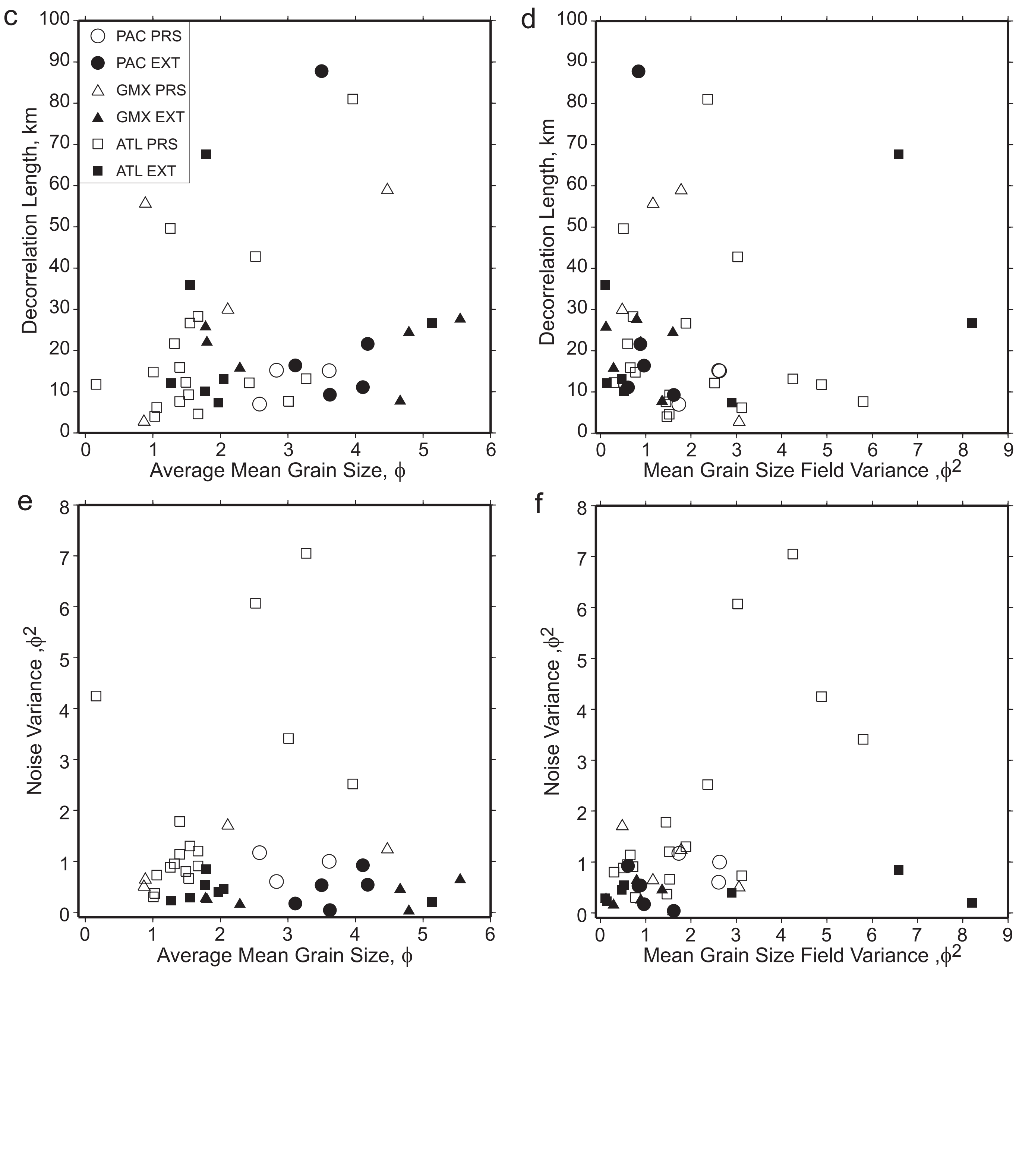

Figure 12 cont.

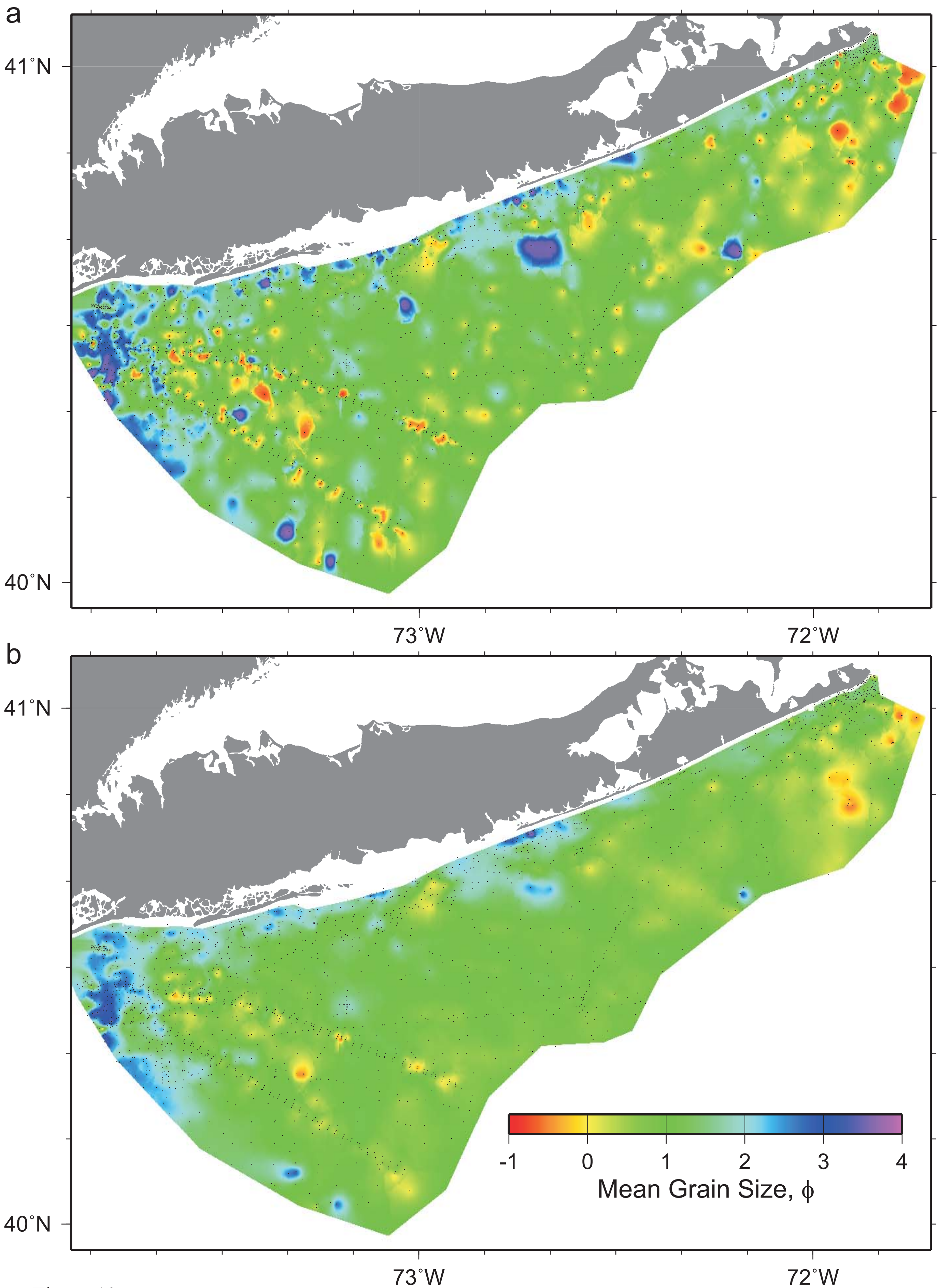

Figure 13

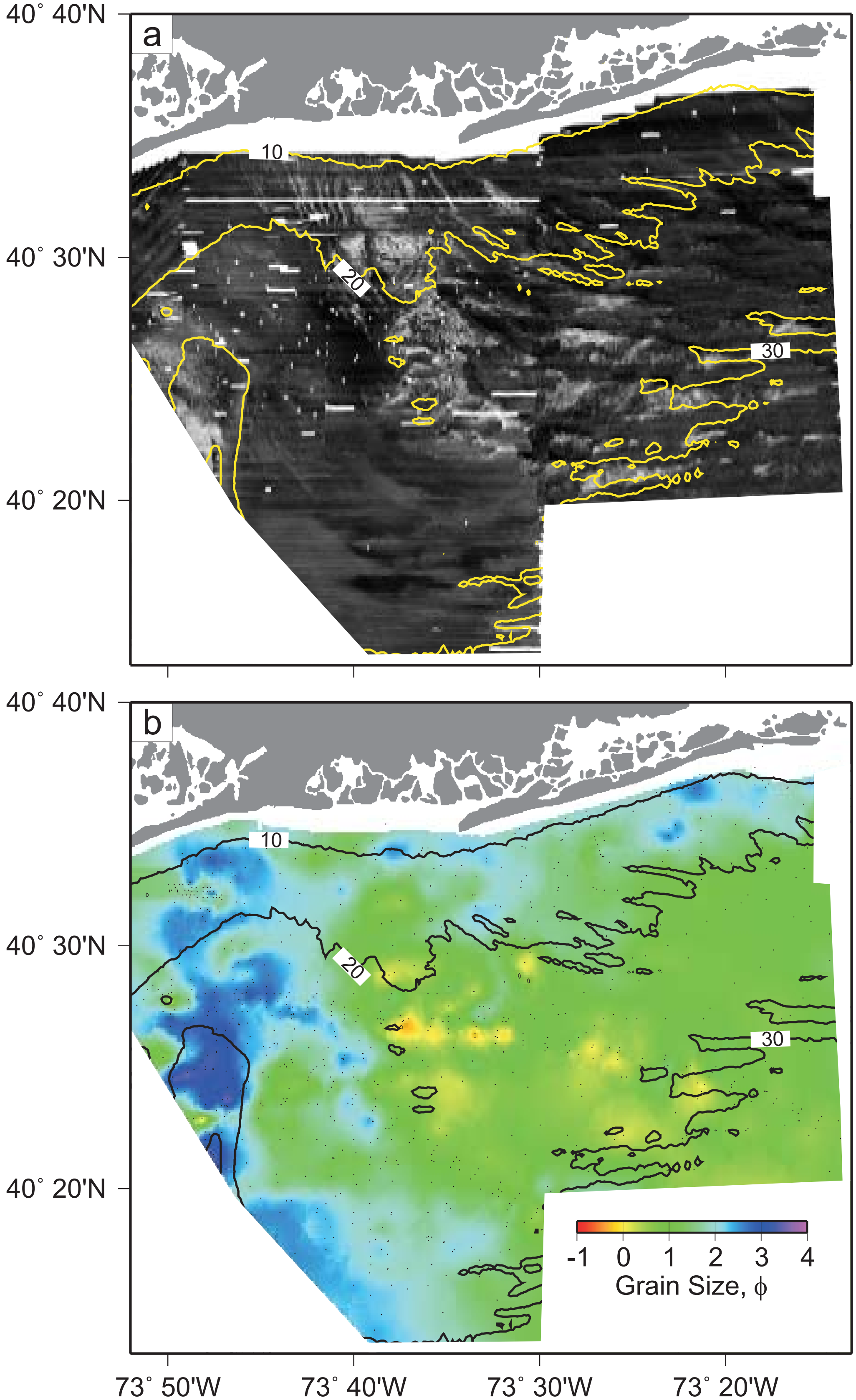

40° 40'N
40° 30'N
40° 20'N
a
10
20
30
40° 40'N
40° 30'N
40° 20'N
b
10
20
30
-1
0
1
2
3
4
Grain Size, ϕ
73° 50'W
73° 40'W
73° 30'W
73° 20'W

Figure 14

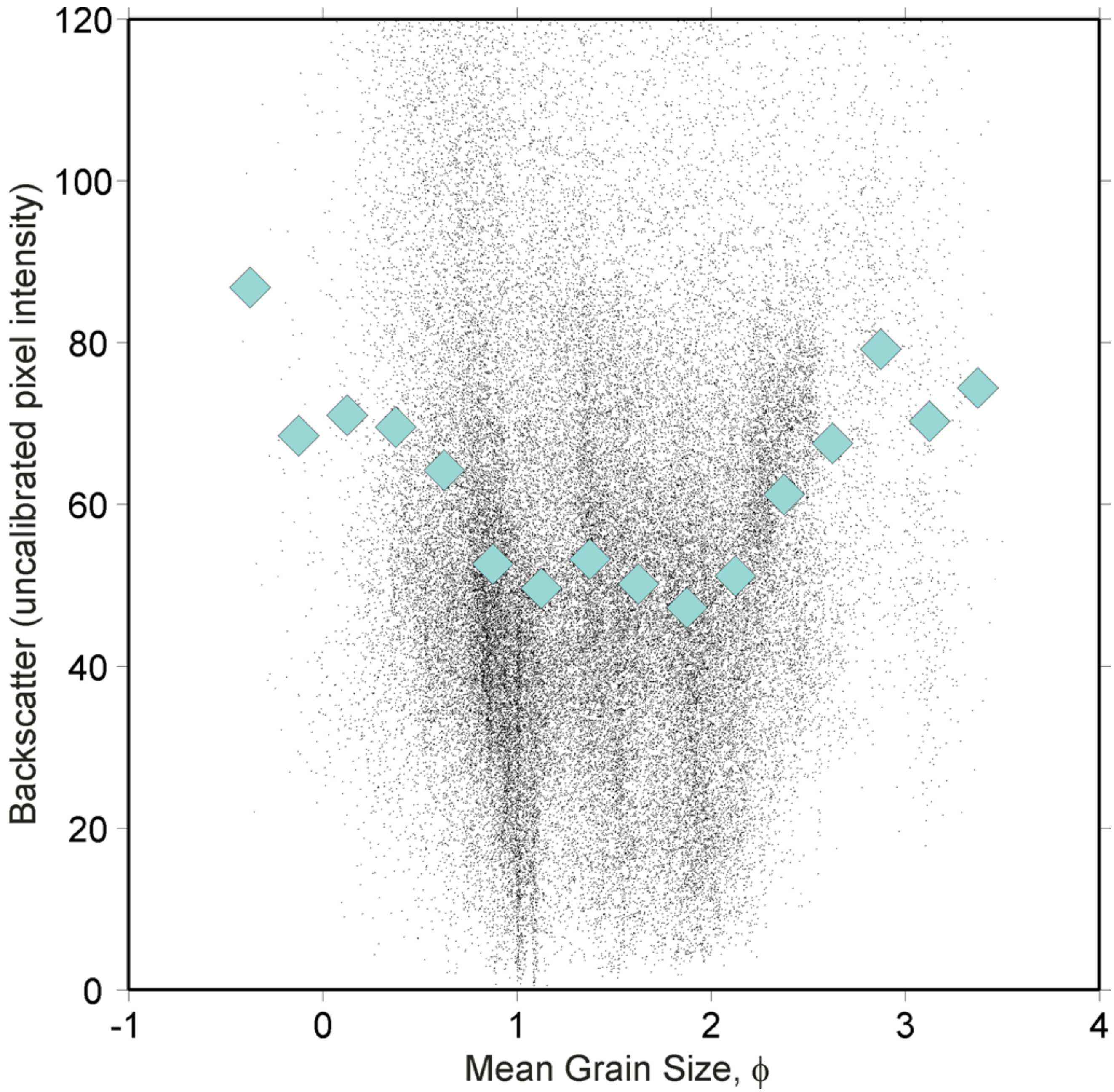
120
100
80
60
40
20
0
-1
0
1
2
3
4
Backscatter (uncalibrated pixel intensity)
Mean Grain Size, ϕ

Figure 15